

1 Comments to the Author:

2 The authors have addressed all comments. At this point, there is only minor  
3 editorial work remaining, as follows.

4 We thank the reviewer for his/her further comments on the improvement of the  
5 manuscript.

6

7 Throughout manuscript: change “foot” of the mountain with “base” and  
8 re-assess the use of “due to” throughout the manuscript.

9 **Reply:** Thanks for the comment. The “foot” of the mountain has been changed  
10 with “base” throughout the whole manuscript. For details, please refer to Line 3  
11 Page 2, Lines 10 and 26 Page 5, Line 15 Page 24, Line 9 Page 26 and Line 4  
12 Page 30 in the revised manuscript.

13 Furthermore, the use of “due to” has been re-assessed and revised  
14 accordingly throughout the manuscript, in addition to those suggested in the  
15 following specific comments. For details, please refer to Line 16 Page 2, Lines  
16 3 and 6 Page 3, Lines 7 and 18 Page 6, Line 9 Page 11, Line 22 Page 14, Line  
17 13 Page 19, Lines 15 and 18 Page 20, Line 26 Page 23, Line 14 Page 25, and  
18 Line 24 Page 26 in the revised manuscript.

19

20 P2L2-3: remove the “i.e.,” before the site names – not needed.

21 **Reply:** Thanks for the comment. The text has been deleted as suggested. For  
22 details, please refer to Lines 2-3, Page 2 in the revised manuscript.

23

24 P2L15: Revise the following sentence “On the other hand, alkyl nitrates at  
25 TMS were...” to something like the following: “In contrast to TW, the alkyl  
26 nitrate levels measured at TMS mainly resulted from the photo- oxidation of  
27 the parent hydrocarbons at TW during mesoscale circulation, i.e., valley  
28 breezes, corresponding to 52-86% of the alkyl nitrate levels at TMS.”

29 **Reply:** The sentence has been revised as above. Please refer to Lines 15-18,  
30 Page 2 in the revised manuscript for details.

31

32 P3L2: change “due to” to “because of”

33 **Reply:** Thanks for the comment. “Due to” has been revised as “because of”.  
34 For details, please refer to Line 3, Page 3 in the revised manuscript.

35

36 P3L6: change “due to” to something like “resulting from”

37 **Reply:** Thanks for the comment. “Due to” has been revised as “resulting from”.  
38 For details, please refer to Line 6, Page 3 in the revised manuscript.

39

40 P5L18: delete “i.e.,” not needed – add comma after (TMS)

41 **Reply:** Thanks for the comment. The “i.e.,” has been deleted as suggested.  
42 For details, please refer to Line 19 Page 5 in the revised manuscript.

1 P5L28: You state that the monitoring site was 15-20 m above the ground –  
2 that’s a pretty significant range. Is there more concise information either about  
3 the station/inlet height to narrow down this range?

4 **Reply:** Thanks for the comment. The monitoring site was approximately 20 m  
5 above ground level. The text has been revised accordingly. For details, please  
6 refer to Line 30, Page 5 in the revised manuscript.

7  
8 P8L1: Please introduce CO, NO, NO<sub>2</sub> and NO<sub>x</sub> – this is the first time these  
9 have been presented in the manuscript.

10 **Reply:** Thanks for the comment. The detailed information of CO, NO, NO<sub>2</sub> and  
11 NO<sub>x</sub> has been provided. For details, please refer to Lines 1-2, Page 8 in the  
12 revised manuscript.

13  
14 P8L6: “baseline” should be change to “background”

15 **Reply:** “baseline” has been changed to “background”. For details, please refer  
16 to Line 9, Page 8 in the revised manuscript.

17  
18 P8L10-16: The following sentence is confusing – first off how often were each  
19 of the different analyzers calibrated? Regarding the “other” analyzers, it says  
20 they were calibrated “daily” using scrubbed ambient air – this would be zeroed,  
21 not calibrated. The way this is written, the “other” analyzers are only calibrated  
22 weekly, but zeroed daily, and we are not provided the information on the  
23 temporal calibrations of the ozone analyzer. Please revise to state the  
24 frequency of the zeros and calibrations for each of the instruments. The O<sub>3</sub>  
25 analyzer was calibrated (how often, hourly, daily, weekly?) by using a transfer  
26 standard (Thermo Environmental Instruments (TEI) 49PS), while the other  
27 analyzers were calibrated daily by analyzing scrubbed ambient air (this is  
28 zeroing the analyzer) (TEI, Model 111) and a span gas mixture weekly with a  
29 NIST (National Institute of Standards and Technology) traceable standard  
30 which was diluted to representative mixing ratios using a dynamic calibrator  
31 (EnviroNics, Inc., Model 15 6100).

32 **Reply:** Thanks for the comment. The above sentences have been revised as  
33 follows:

34 “The O<sub>3</sub> analyzer was calibrated weekly by using a transfer standard (Thermo  
35 Environmental Instruments (TEI) 49 PS), while the other analyzers were  
36 zeroed daily by analyzing scrubbed ambient air and calibrated weekly by a  
37 span gas mixture with a NIST (National Institute of Standards and Technology)  
38 traceable standard which was diluted to representative mixing ratios using a  
39 dynamic calibrator (EnviroNics, Inc., Model 6100).”

40 For details, please refer to Lines 13-18, Page 8 in the revised manuscript.

41  
42 P9L17: It’s hard to tell in the pdf version, but this should be the beginning of a  
43 new paragraph.

44 **Reply:** Sorry for the confusion. Indeed, it was the beginning of a new

1 paragraph in the manuscript (in word version). For details, please refer to Line  
2 20 Page 9 in the revised manuscript. To make it clearer, 2 characters were  
3 indented for the first line of each paragraph throughout the manuscript.

4  
5 P12 Table 1 (and also S1): it would be useful to either include 10th and 90th  
6 percentiles or quartiles (or both) to the statistics – this allows the reader to  
7 better assess the variability in the data and between sites.

8 **Reply:** Thanks for the great comment. 10<sup>th</sup> and 90<sup>th</sup> percentiles for the data  
9 have been added in Table 1 and Table S1. For details, please refer to Table 1  
10 in the revised manuscript and Table S1 in the revised supplementary.

11  
12 P13L19-21: Revise to the following: High mixing ratios of O<sub>3</sub> and alkyl nitrates  
13 were usually associated with meteorological conditions with high-pressure  
14 system and/or stable conditions, such as high temperatures, intense solar  
15 radiation and low wind speeds.

16 **Reply:** Thanks for the comment. The sentence has been revised accordingly.  
17 For details, please refer to Lines 24-27, Page 13 in the revised manuscript.

18  
19 P13L27: delete “well” The maximum values were comparable and the diurnal  
20 patterns well tracked each...

21 **Reply:** It has been deleted. For details, please refer to Line 4, Page 14 in the  
22 revised manuscript.

23  
24 P14L1: add “the” other for the C<sub>3</sub>-C<sub>4</sub> alkyl nitrates...

25 **Reply:** The word has been added in the revised manuscript. Please refer to  
26 Line 5, Page 14 in the revised manuscript.

27  
28 P14L5: delete “respectively”

29 **Reply:** The word has been deleted in the revised manuscript. Please refer to  
30 Line 9, Page 14 in the revised manuscript.

31  
32 P14L6: simply say “high O<sub>3</sub> days” so the sentence reads more fluidly (not  
33 high-level)

34 **Reply:** The text has been revised accordingly. Please refer to Line 10, Page  
35 14 in the revised manuscript.

36  
37 P14L19: States that the elevated levels of MeONO<sub>2</sub> and EtONO<sub>2</sub> are “likely  
38 indicative of photo-oxidation of methane and ethane”. Please provide an  
39 estimate on this point as the lifetime of methane and ethane are sufficiently  
40 long that local production usually isn’t dominate for these two gases.

41 **Reply:** Thanks for pointing this out. The high levels of MeONO<sub>2</sub> and EtONO<sub>2</sub>  
42 observed at around noon were likely resulted from regional transport and/or  
43 mesoscale circulation, which were further analyzed in Section 3.2.3. Therefore,  
44 the text has been revised as follows:

1 "...likely resulted from regional transport (Guo et al., 2009; Jiang et al., 2010)  
2 and/or mesoscale circulations (Gao et al., 2005; Wang et al., 2006) (Section  
3 3.2.3)"

4 For details, please refer to Lines 23-24, Page 14 in the revised manuscript.

5

6 P14L26: Revise this to say that "...the high levels of MeONO<sub>2</sub> and EtONO<sub>2</sub> are  
7 likely related to marine..."

8 **Reply:** Thanks for the comment. The text has been revised as suggested. For  
9 details, please refer to Line 29, Page 14 in the revised manuscript.

10

11 P16L6: replace "helpful" with "valuable"

12 **Reply:** "helpful" has been replaced by "valuable". For details, please refer to  
13 Line 9, Page 16 in the revised manuscript.

14

15 P16L21: Introduce Eq. 1 – currently, it simply resides in the text with no  
16 reference to it.

17 **Reply:** Thanks for pointing this out. "Eq.1" has been revised as "Equation 1".  
18 For details, please refer to Line 24, Page 16 in the revised manuscript.

19

20 P16L26: revise to "...processing, respectively; [OH] is the..."

21 **Reply:** The text has been revised as above. For details, please refer to Line 29,  
22 Page 16 in the revised manuscript.

23

24 P17L8: delete "most"

25 **Reply:** The text has been deleted. For details, please refer to Line 10, Page 17  
26 in the revised manuscript.

27

28 P17L17: Delete "[OH]": The diurnal average OH mixing ratios [OH] were

29 **Reply:** The text has been deleted. For details, please refer to Line 20, Page 17  
30 in the revised manuscript.

31

32 P17,L20: Revise to: "...because the other parameters (k<sub>A</sub>, k<sub>B</sub>, α<sub>1</sub>, α<sub>2</sub> and  
33 JRONO<sub>2</sub>) were obtained from the literatures..." Note: literature should not be  
34 plural.

35 **Reply:** Thanks for the comment. The "literatures" has been revised as  
36 "literature". For details, please refer to Line 23, Page 17 in the revised  
37 manuscript.

38

39 P19L13-18: First, the following should be revised: "...due to long atmospheric  
40 lifetimes and slow photochemical degradation rates of methane and ethane..."  
41 to something as: "...resulting from their relatively long atmospheric lifetimes  
42 and the slow photochemical reaction rates of methane and ethane..."  
43 Moreover, this goes back to P14L19, which suggested that the elevated  
44 MeONO<sub>2</sub> and EtONO<sub>2</sub> are a result of photochemistry – these sections can be

1 construed as contradictory. Please reconcile the discussion on P14 by  
2 including a calculation or revising the text accordingly.

3 **Reply:** Thanks for the comment. The text "...due to long atmospheric lifetimes  
4 and slow photochemical degradation rates of methane and ethane..." has been  
5 revised as suggested. For details, please refer to Lines 13-14, Page 19 in the  
6 revised manuscript.

7 Furthermore, the discussion on P14 has been revised as mentioned above  
8 (Lines 23-24, Page 14).

9

10 P20,L3: Change to "Regarding the C3 alkyl nitrates,..."

11 **Reply:** The text has been changed to "Regarding the C3 alkyl nitrates". For  
12 details, please refer to Line 3, Page 20 in the revised manuscript.

13

14 P20L5: "revealing" isn't a great word choice in this case. Recommend  
15 changing to something like: indicating, demonstrating, etc.

16 **Reply:** The "revealing" has been changed to "indicating". For details, please  
17 refer to Line 5, Page 20 in the revised manuscript.

18

19 P21L25-26: Revise to: "The standard error in Figure 7 were..." Note: error  
20 should not be plural.

21 **Reply:** Thanks for the comment. The text has been revised as "The standard  
22 error in Figure 7 was...". For details, please refer to Lines 25-26, Page 21 in  
23 the revised manuscript.

24

25 P21L26-29: Revise the following: Since the air masses arriving at TMS were  
26 photochemically aged (Guo et al., 2013a), the original source profiles of alkyl  
27 nitrates and their parent hydrocarbons were altered at this mountain site." to  
28 something like:

29 "The source profiles of the alkyl nitrates and their parent hydrocarbons were  
30 altered resulting from photochemical transformation during transport to the  
31 TMS site."

32 **Reply:** Thanks for the comment. The sentence has been revised as above.  
33 For details, please refer to Lines 26-28, Page 21.

34

35 P22L2, 8 & 15: change n/i-butane to i/n-butane to be consistent throughout the  
36 manuscript.

37 **Reply:** Thanks for pointing this out. All the "n/i-butane" has been corrected as  
38 "i/n-butane" throughout the manuscript.

39

40 P24L16: As written, this refers to a single forest fire – is this correct or should  
41 this be plural?

42 **Reply:** Yes, the fire should be plural. The text has been revised accordingly.  
43 For details, please refer to Line 16, Page 24 in the revised manuscript.

44

1 P26L1: Delete “Instead” and start the sentence with “The C3-C4...” or say  
2 something such as: “In contrast to the C1 and C2 alkyl nitrates,...”

3 **Reply:** The text has been revised as suggested. For details, please refer to  
4 Line 1, Page 26 in the revised manuscript.

5  
6 P26L8: Replace “brought” with “transported”

7 **Reply:** “brought” has been replaced by “transported”. For details, please refer  
8 to Line 8, Page 26 in the revised manuscript.

9  
10 P26L22-23: for the following: “...photochemical formation of alkyl nitrates was  
11 occurring, and eventually contributed to the ambient levels of alkyl nitrates at  
12 TMS.” either delete the part of the sentence after the comma or revise as  
13 follows: “...photochemical formation of alkyl nitrates was occurring, contributing  
14 to their ambient levels at TMS.”

15 **Reply:** Thanks for the comment. The sentence has been revised as  
16 “...contributing to their ambient levels at TMS”.

17 For details, please refer to Lines 22-23, Page 26 in the revised manuscript.

18  
19 P27L4-8: For the following: The results demonstrated that when there was  
20 mesocale circulation, the levels of alkyl nitrates at TMS were dominated by the  
21 photo-oxidation of their parent hydrocarbons originated from the urban site  
22 TW, one possible reason leading to similar levels of alkyl nitrates at the two  
23 sites, though the values of their parent hydrocarbons were lower at TMS.  
24 Revise to something like: These results demonstrate that when there was  
25 mesocale circulation, the alkyl nitrate levels at TMS were dominated by the  
26 photo-oxidation of their parent hydrocarbons that originated from the urban  
27 site TW. Although the mixing ratios of the parent hydrocarbons were lower at  
28 TMS, this is still one possible explanation leading to the similar levels of alkyl  
29 nitrates measured at the two sites.

30 **Reply:** Thanks for the comment. The sentence has been revised as follows:  
31 “These results demonstrate that when there was mesoscale circulation, the  
32 alkyl nitrate levels at TMS were dominated by the photo-oxidation of their  
33 parent hydrocarbons that originated from the urban site TW. Although the  
34 mixing ratios of the parent hydrocarbons were lower at TMS, this is still one  
35 possible explanation leading to the similar levels of alkyl nitrates measured at  
36 the two sites.”

37 For details, please refer to Lines 4-9, Page 27 in the revised manuscript.

38  
39 P27,L24: change to “...alkyl nitrates measured at TMS.”

40 **Reply:** The text has been revised accordingly. For details, please refer to Line  
41 25, Page 27 in the revised manuscript.

42  
43 P27L26: change “...in the...” to “...for the...”

44 **Reply:** “in” has been changed to “for”. For details, please refer to Line 27,

1 Page 27 in the revised manuscript.

2

3 P28,L20-21: For the following: In addition, as the formation of alkyl nitrates  
4 consumes NO, it resulted in negative contribution to O3 formation.

5 Change to: Additionally, as the formation of alkyl nitrates consumes NO, this  
6 process results in a negative contribution to O3 formation.

7 **Reply:** The sentence has been revised as suggested above. For details,  
8 please refer to Lines 21-22, Page 28 in the revised manuscript.

9

10 P29L20: Change: "The results..." to "These results..."

11 **Reply:** "The results..." has been revised as "These results...". For details,  
12 please refer to Line 22, Page 29 in the revised manuscript.

13

14 P30L19: change "...led to the..." to "...resulted in..."

15 **Reply:** "...led to the..." has been changed to "...resulted in...". For details,  
16 please refer to Line 19, Page 30 in the revised manuscript.

17

18 Figure S1: Change to sans serif font and adjust the colors so TW is red to be  
19 consistent with the rest of the manuscript.

20 **Reply:** The reviewer's comment is highly appreciated. In fact, there was no  
21 sans serif font in the software we used to draw the figure, we have changed  
22 the font to be "Arial". Furthermore, to present the figure more clearly, the font  
23 size has been increased. Additionally, the colors for TW have been changed to  
24 be red. For details, please refer to Figure S1 in the revised supplementary.

25

26 Figure S2: Is it possible to increase the clarity of the labels on the weather  
27 charts?

28 **Reply:** Thanks for the comment. The clarity of the labels on the weather charts  
29 has been improved. Please refer to Figure S2 for details.

30

31

32

33

34

35

36

37

38

39

40

41

42

43

44

1 **New insight into the spatiotemporal variability and source apportionments of**  
2 **C<sub>1</sub>-C<sub>4</sub> alkyl nitrates in Hong Kong**

3 Z.H. Ling<sup>1,2</sup>, H. Guo<sup>2\*</sup>, I.J. Simpson<sup>3</sup>, S.M. Saunders<sup>4</sup>, S.H.M. Lam<sup>4,5</sup>, X.P. Lyu<sup>2</sup>, D.R.  
4 Blake<sup>3</sup>

5 <sup>1</sup> School of Atmospheric Sciences, Sun Yat-sen University, Guangzhou, China

6 <sup>2</sup> Air Quality Studies, Department of Civil and Environmental Engineering, The Hong  
7 Kong Polytechnic University, Hong Kong

8 <sup>3</sup> Department of Chemistry, University of California at Irvine, California, USA

9 <sup>4</sup> School of Chemistry and Biochemistry, University of Western Australia, Perth,  
10 Western Australia, Australia

11 <sup>5</sup> Pacific Environment Limited, Perth, Western Australia, Australia

12

13 \* Corresponding author. Tel: +852 34003962. Fax: +852 23346389. Email:  
14 [ceguohai@polyu.edu.hk](mailto:ceguohai@polyu.edu.hk)

15



## 1 Abstract

2 C<sub>1</sub>-C<sub>4</sub> alkyl nitrates (RONO<sub>2</sub>) were measured concurrently at a mountain site, Mt.  
3 Tai Mo Shan (TMS), and an urban site, Tsuen Wan (TW) at the base of the same  
4 mountain in Hong Kong from September to November 2010. Although the levels of  
5 parent hydrocarbons were much lower at TMS ( $p < 0.05$ ), similar alkyl nitrate levels  
6 were found at both sites regardless of the elevation difference, suggesting various  
7 source contributions of alkyl nitrates at the two sites. Prior to using a positive matrix  
8 factorization (PMF) model, the data at TW were divided into “meso” and “non-meso”  
9 scenarios for the investigation of source apportionments with the influence of  
10 mesoscale circulation and regional transport, respectively. Secondary formation was  
11 the prominent contributor of alkyl nitrates in the “meso” scenario ( $60 \pm 2\%$ ,  $60.2 \pm$   
12  $1.2$  pptv), followed by biomass burning and oceanic emissions, while biomass burning  
13 and secondary formation made comparable contributions to alkyl nitrates in the  
14 “non-meso” scenario, highlighting the strong emissions of biomass burning in the  
15 inland Pearl River Delta (PRD) region. In contrast to TW, the alkyl nitrate levels  
16 measured at TMS mainly resulted from the photo-oxidation of the parent  
17 hydrocarbons at TW during mesoscale circulation, i.e., valley breezes, corresponding  
18 to 52-86% of the alkyl nitrate levels at TMS. Furthermore, regional transport from the  
19 inland PRD region made significant contributions to the levels of alkyl nitrates  
20 (~58-82%) at TMS in the “non-meso” scenario, resulting in similar levels of alkyl  
21 nitrates observed at the two sites. The simulation of secondary formation pathways  
22 using a photochemical box model found that the reaction of alkyl peroxy radicals  
23 (RO<sub>2</sub>) with nitric oxide (NO) dominated the formation of RONO<sub>2</sub> at both sites, and the  
24 formation of alkyl nitrates contributed negatively to O<sub>3</sub> production, with average  
25 reduction rates of 4.1 and 4.7 pptv/pptv at TMS and TW, respectively.

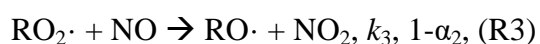
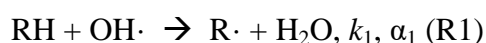
26  
27 **Key word:** Alkyl nitrates; Source apportionment; Secondary formation; Biomass  
28 burning

29

## 1 **1. Introduction**

2 Alkyl nitrates (RONO<sub>2</sub>) are important photochemical pollutants in the  
3 atmosphere **because of** their roles in local, regional and global atmospheric chemistry  
4 (Jenkin et al., 2000; Seinfeld and Pandis, 2006). Alkyl nitrates are reactive nitrogen  
5 compounds (NO<sub>y</sub>) and act as a critical reservoir of nitrogen oxides (NO<sub>x</sub> = NO + NO<sub>2</sub>)  
6 during long-range transport **resulting from** their relatively low reactivity (Atkinson,  
7 2006).

8 A number of studies conducted in different environments have shown that alkyl  
9 nitrates are either emitted from marine sources directly and/or produced indirectly  
10 through photochemical reactions (Roberts et al., 1998; Blake et al., 2003; Simpson et  
11 al., 2002, 2003, 2006; Reeves et al., 2007; Wang et al., 2013). In the case of biomass  
12 burning, secondary alkyl nitrate formation is believed to occur by the photo-oxidation  
13 of emitted hydrocarbons with a formation mechanism of RO and NO<sub>2</sub> (Simpson et al.,  
14 2002). The photochemical pathways for the secondary formation of alkyl nitrates are  
15 expressed as follows (Atkinson et al., 2006; Jenkin et al., 2000; Arey et al., 2001;  
16 Sommariva et al., 2008):

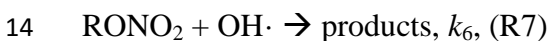


22 where  $k_1, k_2, k_3, k_4$  and  $k_5$  are reaction rate constants.  $\alpha_1$  and  $\alpha_2$  are branching  
23 ratios for the corresponding radicals, which increase as the carbon number increases  
24 and are dependent on the carbon chain length.

25 Photochemical formation of alkyl nitrates influences the oxidation of NO to NO<sub>2</sub>,  
26 subsequently leading to O<sub>3</sub> production by NO<sub>2</sub> photolysis. Therefore, alkyl nitrates are  
27 often used as indicators of photochemical O<sub>3</sub> production (Simpson et al., 2006).  
28 Furthermore, the interactions of alkyl nitrates with their parent hydrocarbons provide  
29 useful information about the photochemical processing of air masses. Comparing  
30 measured and predicted RONO<sub>2</sub>/RH ratios calculated using the laboratory kinetic data

1 as a function of time, Bertman et al. (1995) examined the photochemical evolution of  
2 alkyl nitrates at Scotia, Pennsylvania and the Kinterbish Wildlife Area, Alabama.  
3 Since then, this approach has been used to investigate the evolution of alkyl nitrates  
4 with air mass age in different regions (Simpson et al., 2006; Reeves et al., 2007;  
5 Russo et al., 2010; Worton et al., 2010; Wang et al., 2013). Fairly good agreement  
6 ( $>0.5$ ) between measured and modeled ratios suggests that the oxidation of  
7 single-parent hydrocarbons represents the evolution of their daughter alkyl nitrates,  
8 while poor correlation indicated sources other than photochemical formation of alkyl  
9 nitrates.

10 In contrast, the main sinks for ambient alkyl nitrates are photolysis and reactions  
11 with hydroxyl radical (OH), making alkyl nitrate lifetimes vary with season, latitude  
12 and altitude (days to weeks):



15 where  $h\nu$  is sunlight and  $J_{\text{RONO}_2}$  and  $k_6$  are the photolysis and OH reaction rate  
16 constants, respectively. The importance of alkyl nitrate removal by photolysis  
17 decreases as the carbon number increases (Clemitshaw et al., 1997; Talukdar et al.,  
18 1997). Dry deposition has recently been recognized as another pathway for the  
19 removal of atmospheric alkyl nitrates (Russo et al., 2010; Wu et al., 2011).

20 Despite increased concern over photochemical pollution in Hong Kong and the  
21 greater Pearl River Delta (PRD) region, limited studies have focused on the  
22 characteristics of alkyl nitrates, which share a common mechanism with  
23 photochemical  $\text{O}_3$  formation and act as indicators of photochemical processing. For  
24 example, based on measurements conducted in 2001-2002, including during ozone  
25 episodes, Simpson et al. (2006) analyzed the general characteristics of alkyl nitrates at  
26 a coastal site (Tai O) in Hong Kong.  $\text{C}_3$ - $\text{C}_4$  alkyl nitrates were the most abundant  
27 species, with maximum and minimum levels in winter and summer, respectively. The  
28 diurnal variations suggested that photochemical production was the dominant source  
29 of alkyl nitrates at Tai O. Furthermore, through approximate calculations, it was  
30 concluded that the methoxy radical ( $\text{CH}_3\text{O}\cdot$ ) reaction with  $\text{NO}_2$  was a viable

1 alternative pathway for the observed high levels of MeONO<sub>2</sub> during pollution  
2 episodes. This mechanism was subsequently verified by Archibald et al. (2007) via  
3 box model simulations, whereby RO + NO<sub>2</sub> → RONO<sub>2</sub> became important for  
4 MeONO<sub>2</sub> formation at 10 ppb NO<sub>2</sub> and dominant at 35 ppb NO<sub>2</sub>. However,  
5 knowledge related to the chemical evolution and source apportionments of individual  
6 alkyl nitrates and their relationship with parent hydrocarbons is still lacking in Hong  
7 Kong, especially given that levels of alkyl nitrate precursors have varied since 2002  
8 (Ling and Guo 2014). Hence, in this study, intensive field measurements of C<sub>1</sub>-C<sub>4</sub>  
9 alkyl nitrates were conducted at two sites - a mountain site (Mt. Tai Mo Shan, TMS)  
10 and an urban site (Tsuen Wan, TW) at the base of the same mountain in Hong Kong.  
11 The data were analyzed and compared with the previous study conducted at Tai O  
12 (Simpson et al., 2006). The aims were to investigate the spatiotemporal variations and,  
13 for the first time, source apportionments and photochemical formation pathways and  
14 evolution of alkyl nitrates in Hong Kong.

15

## 16 **2. Methodology**

### 17 **2.1. Sampling sites**

18 In this study, concurrent field measurements were conducted at two sites located  
19 at different elevations of the highest mountain, Mt. Tai Mo Shan (TMS) with an  
20 elevation of 957 m a.s.l. in Hong Kong from September 6 to November 29, 2010. A  
21 detailed description of the topography of Mt. TMS was provided in an overview paper  
22 (Guo et al., 2013a). In brief, Figure 1 presents the two sampling locations and the  
23 surroundings. The high-elevation site (TMS) was set on the rooftop of a building on  
24 the mountainside (640 m a.s.l.), the highest logistically feasible observation location,  
25 beyond which the area comprised the natural landscape with shrubs and grasses to the  
26 mountain summit (AFCD, 2008). The measurement site at the base of the mountain  
27 was the monitoring station of the Hong Kong Environmental Protection Department  
28 (HKEPD) at Tsuen Wan (TW), a mixed residential, commercial and light industrial  
29 area in the New Territories of Hong Kong. The TW monitoring site was located on the  
30 rooftop of a building, approximately 20 m above ground level. The linear distance

1 between the TMS and TW sites was about 7 km and the difference in elevation  
2 between the two sites was 630 m. In general, the solar radiation was comparable at the  
3 two sites, while the temperature was higher and the relative humidity and wind speed  
4 were lower at the TW site (Guo et al., 2013a). The winds at TMS were generally from  
5 the north with speeds ranging from 0.02 to 4 m s<sup>-1</sup>, and the winds at TW were  
6 predominantly from the southeast at speeds of 1-3 m s<sup>-1</sup> with easterly winds at night  
7 and southerly winds during the day. Because of its unique topography, the air at TMS  
8 was often influenced by the mountain-valley breezes and regional transport (Guo et  
9 al., 2013a). Based on the average wind speed of 1.9 m/s, air masses transported from  
10 upwind locations, on both local (~7 km) and regional scales (~20 km), took  
11 approximately 1-3 hours to arrive at the TMS site (Guo et al., 2012, 2013a).

12 The Tai O sampling station was a rural/coastal site located on the western coast  
13 of Lantau Island in southwestern Hong Kong (elevation, 80 m a.s.l.) (Figure 1). This  
14 site overlooks the Pearl River Estuary to the west and north, and the South China Sea  
15 to the south. It is 32 km away from the urban center to the east and about the same  
16 distance from Macau/Zhuhai to the west. Major man-made sources in the region are  
17 located to the east, north and southwest. Local emissions are small because of a sparse  
18 population and light traffic. Owing to Asian Monsoon circulation, this site is  
19 frequently affected by polluted continental air masses from the highly industrialized  
20 PRD region of mainland China in cold seasons. A detailed description of the site is  
21 provided in Wang et al. (2003).



22  
23 Figure 1. Tai Mo Shan (TMS) and Tsuen Wan (TW) sampling sites and the  
24 surrounding environments in Hong Kong.

## 2.2. Sampling and analysis of volatile organic compounds (VOCs)

Whole air samples were collected on 10 O<sub>3</sub> episode days and 10 non-O<sub>3</sub> episode days using evacuated 2-L stainless steel canisters. Each of the collected canister samples was integrated over a 60-min sampling period. A total of 384 samples were collected at the two sites. The O<sub>3</sub> episode days were selected as the days with the highest daytime hourly O<sub>3</sub> level at a regional scale (higher than 100 ppbv), which were based on weather forecasts and meteorological data analysis, and confirmed by the observed O<sub>3</sub> mixing ratios. During non-O<sub>3</sub> episode days, one-hour integrated samples were collected at 2-h intervals from 0700 to 1900 local time (LT) (7 samples per day). On O<sub>3</sub> episode days, one-hour integrated samples were collected from 0900 to 1600 LT at 1-h intervals with additional integrated samples collected at 1800, 2100, 0000, 0300 and 0700 LT (a total of 13 samples per day). After the campaign, the canister samples were sent to the University of California, Irvine (UCI) for chemical analysis. Other studies have provided detailed descriptions of the analytical system and the quality control, detection limits and analysis precision of the VOC samples (Simpson et al., 2006, 2010). In brief, the precision and detection limit of the alkyl nitrate measurements is 5% and 0.02 pptv, respectively. The calibration scale for the alkyl nitrate measurements changed in 2008, increasing by factors of 2.13, 1.81, 1.24 and 1.17 for the C<sub>1</sub>, C<sub>2</sub>, C<sub>3</sub> and C<sub>4</sub> alkyl nitrates, respectively (Simpson et al., 2011). In other words, the alkyl nitrates reported at Tai O by Simpson et al. (2006) were lower than the data reported here, and the Tai O data have been adjusted to the new calibration scale to allow direct comparison with this work. The Tai O sampling campaign was conducted from 24 August 2001 to 31 December 2002. Different from the air samples collected at TMS and TW, each whole-air sample at Tai O was collected for only 1-min, and was then analyzed at UCI. Intensive sampling from 0700-1900 LT was conducted every 2-h during the selected pollution episodes (17-19 October 2001, 29-30 August, 5-6 September, 9-11 and 25 October, 6-8 and 12 November 2002). Apart from the intensive sampling days, samples were taken either daily or every few days, typically in the midafternoon (Simpson et al., 2006).

1 | **2.3. Continuous measurements of O<sub>3</sub>, carbon monoxide (CO) and nitric oxide –**  
2 | **nitrogen dioxide – nitrogen oxides (NO-NO<sub>2</sub>-NO<sub>x</sub>)**

3 | At TMS, online measurements of O<sub>3</sub>, CO and NO-NO<sub>2</sub>-NO<sub>x</sub> were made using  
4 | commercial analyzers. Ozone was measured using a commercial UV photometric  
5 | instrument (Advanced Pollution Instrumentation (API), model 400E) that has a  
6 | detection limit of 0.6 ppbv. Carbon monoxide was measured with a gas filter  
7 | correlation, nondispersive infrared analyzer (API, Model 300E) with a heated  
8 | catalytic scrubber (as purchased) to convert CO to carbon dioxide (CO<sub>2</sub>) for  
9 | background determination. The detection limit was 30 ppbv for a 2-min average. The  
10 | 2σ precision was about 1% for a level of 500 ppbv (2-min average) and the overall  
11 | uncertainty was estimated to be 10%. NO, NO<sub>2</sub> and NO<sub>x</sub> were detected with a  
12 | chemiluminescence NO-NO<sub>2</sub>-NO<sub>x</sub> analyzer (API, Model 200E) that had a detection  
13 | limit of 0.5 ppbv. The O<sub>3</sub> analyzer was calibrated weekly by using a transfer standard  
14 | (Thermo Environmental Instruments (TEI) 49 PS), while the other analyzers were  
15 | zeroed daily by analyzing scrubbed ambient air and calibrated weekly by a span gas  
16 | mixture with a NIST (National Institute of Standards and Technology) traceable  
17 | standard which was diluted to representative mixing ratios using a dynamic calibrator  
18 | (EnviroNics, Inc., Model 6100). The Standard (Scott-Marrin, Inc.) contained 156.5  
19 | ppmv CO (±2%), 15.64 ppmv SO<sub>2</sub> (±2%), and 15.55 ppmv NO (±2%). For the O<sub>3</sub>,  
20 | CO, NO and NO<sub>x</sub> analyzers, a data logger (Environmental Systems Corporation  
21 | Model 8816) was used to control the calibrations and to collect 1-minute data.

22 | In addition to the above chemical measurements, several meteorological  
23 | parameters, including wind speed and direction, temperature, relative humidity and  
24 | solar radiation, were measured by the integrated sensor suite (Vantage Pro TM &  
25 | Vantage Pro 2 Plus TM Weather Stations, Davis Instruments).

26 | At TW, hourly O<sub>3</sub>, CO, NO-NO<sub>2</sub>-NO<sub>x</sub> and meteorological data were obtained  
27 | from the HKEPD (<http://epic.epd.gov.hk/ca/uid/airdata>). The hourly data were derived  
28 | by averaging 1-min data subsequently over the same time interval as the TMS data.  
29 | Detailed information about the measurements, quality assurance and control protocols  
30 | can be found in the HKEPD report (HKEPD, 2012). In addition, Table S1 in the

1 supplementary information shows descriptive statistics of main non-methane  
2 hydrocarbons (NMHCs) and trace gases at both sites, while Figure S1 presents the  
3 time series of trace gases and meteorological parameters at the two sites.

#### 4 **2.4. Positive Matrix Factorization (PMF) model**

5 In this study, the US EPA PMF 3.0  
6 (<http://www.epa/heads/products/pmf/pmf.html>) was used for the source  
7 apportionments of the observed alkyl nitrates at TW. Our previous studies provided  
8 detailed information about the PMF model (Ling et al., 2011; Ling and Guo, 2014). In  
9 terms of the PMF input, the uncertainty for each species was determined as the sum of  
10 10% of the VOC concentration and two times the method detection limit (MDL) of  
11 the species (Paatero, 2000). Tracers for different sources were selected for the model  
12 input. For example, CO, ethane and ethyne were the tracers of combustion processes,  
13 and CH<sub>3</sub>Cl was specifically used for biomass burning. DMS was a typical tracer for  
14 marine emissions, while O<sub>x</sub> (*i.e.*, O<sub>3</sub> + NO<sub>2</sub>) was used as the tracer of secondary  
15 formation through photochemical reactions, including the formation of alkyl nitrates,  
16 because O<sub>3</sub> shares a common photochemical source with alkyl nitrates (Simpson et al.,  
17 2006). In addition to the aforementioned species, alkyl nitrate precursors, including  
18 methane, ethane, propane and *i/n*-butanes, were input into the model. In total, sixteen  
19 compounds were used for the model input.

20 Various checks and sensitivity tests were conducted to examine the model  
21 performance. Firstly, many different starting seeds were tested and no multiple  
22 solutions were found. Secondly, the correlation between the predicted and measured  
23 concentration of each species was fairly good at TW ( $R^2=0.64\sim 0.94$ ) after the PMF  
24 implementation. Thirdly, the scale residuals, which are the uncertainty over the  
25 different runs for the input species, ranged between -3 and 3 for the PMF solution.  
26 Fourthly, the ratios of Q(robust)/Q(true) were close to 1 for 4-factor solution, within  
27 the ranges of 0.97-0.98 at TW, higher than those of 3-factor and 5-factor solutions,  
28 indicating all data points were fit better in the 4-factor solution. Indeed, the extracted  
29 source profiles from the 4-factor solution were the most reasonable. All the factors  
30 were mapped to a base factor in all the 100 runs in the bootstrapped simulation for the



1 four-factor solution, suggesting the solution was stable. Lastly, the G-space plot  
2 extracted from the F-peak model results did not present oblique edges, reflecting that  
3 there was little rotation for the selected solution. Overall, the above features  
4 demonstrated that PMF provided reasonable results for the source apportionment of  
5 alkyl nitrates (Ling et al., 2011; Ling and Guo, 2014).

## 6 **2.5. Photochemical box model incorporating master chemical mechanism** 7 **(PBM-MCM)**

8 A photochemical box model coupled with Master Chemical Mechanism  
9 (PBM-MCM) was used to simulate the in-situ formation of alkyl nitrates at TMS and  
10 TW. The PBM-MCM was developed by assuming that it was a well-mixed box  
11 without the treatment of vertical or horizontal dispersion, and the air pollutants in the  
12 model were homogeneous. For the mechanism coupled in the model, the MCM  
13 (version 3.2) used in this study is a state-of-the-art chemical mechanism, which  
14 describes the degradation of 143 primary VOCs including methane and contains  
15 around 16,500 reactions involving 5900 chemical species (Jenkin et al., 1997, 2003;  
16 Saunders et al., 2003). The measured data, including O<sub>3</sub>, CO, NO<sub>x</sub>, SO<sub>2</sub>, 54 VOCs and  
17 methane, together with the actual meteorological conditions of temperature, relative  
18 humidity and boundary layer in the region, were used to constrain the model. The  
19 photolysis rates of different species in the model were parameterized as suggested by  
20 the previous study (Pinho et al., 2009) using the photon flux determined from the  
21 Tropospheric Ultraviolet and Visible Radiation (v5) model based on the actual  
22 conditions, such as meteorological conditions, location and time period of the field  
23 campaign in Hong Kong (Lam et al., 2013). The model output simulated in-situ  
24 formation of alkyl nitrates and other secondary products as well as the full set of  
25 precursors, radicals and intermediates. To provide robust results from the model  
26 simulation, several measures were adopted for the model development. The detailed  
27 information for the model frameworks, the model development and the evaluation for  
28 the model performance has been reported in our previous studies (Lam et al., 2013;  
29 Ling et al., 2014).

30

### 3. Results and discussion

#### 3.1 Descriptive statistics of alkyl nitrates and their parent hydrocarbons

Table 1 presents the descriptive statistics of alkyl nitrates and their parent hydrocarbons at TMS and TW. Figure 2 compares the levels of alkyl nitrates measured at TMS and TW with those measured in different environments in previous studies. In general, 2-PrONO<sub>2</sub> and 2-BuONO<sub>2</sub> were the most abundant alkyl nitrates at the two sites, consistent with the results observed in different environments (Blake et al., 2003; Simpson et al., 2006; Russo et al., 2010; Wang et al., 2013). The relatively higher levels of 2-PrONO<sub>2</sub> and 2-BuONO<sub>2</sub> were associated with the balance between increased branching ratios for photochemical alkyl nitrate formation and the decreased lifetime of both parent alkanes and alkyl nitrates with increasing carbon number (Arey et al., 2001; Simpson et al., 2006; Russo et al., 2010). In comparison, the levels of MeONO<sub>2</sub>, EtONO<sub>2</sub> and 2-PrONO<sub>2</sub> were slightly higher at TW than at TMS ( $p < 0.05$ ), with average values of  $12.6 \pm 0.5$  (mean  $\pm$  95% confidence interval),  $13.3 \pm 0.6$  and  $26.3 \pm 1.2$  pptv, respectively, at TW. The average mixing ratios of 1-PrONO<sub>2</sub> and 2-BuONO<sub>2</sub> were comparable at the two sites ( $p > 0.05$ ). The results were contradictory to the fact that the mixing ratios of their parent hydrocarbons at TMS were much lower than at TW, highlighting the complexity of sources of alkyl nitrates at both sites.

In comparison with other studies, the average mixing ratios of alkyl nitrates at TMS were much higher than those measured in forested areas in coastal New England (Russo et al., 2010) and in tropospheric air influenced by Asian outflow during the airborne TRACE-P mission (Simpson et al., 2003), where the levels of parent hydrocarbons were also lower. (Note that all of the UCI data shown in Figure 2 were adjusted to UCI's post-2008 alkyl nitrates' calibration scale to enable direct comparison (Simpson et al., 2011). However, the mean mixing ratios of C<sub>1</sub>-C<sub>3</sub> alkyl nitrates were slightly lower and the 2-BuONO<sub>2</sub> mixing ratio was higher at TMS than at Tai O (Table 2), Hok Tsui and in Karachi, Pakistan (Barletta et al., 2002; the Karachi data have also been adjusted to the new UCI alkyl nitrates' calibration scale). The differences among TMS, Tai O and Hok Tsui might result not only from the

1 levels of their parent hydrocarbons, but also from the influence of air masses with  
 2 different photochemical ages and sources (Wang et al., 2003). Furthermore, as  
 3 mentioned in Section 2.2, the sampling method and sampling period at TMS were  
 4 different from those at Tai O and Hok Tsui, where the sampling duration was only  
 5 1-min and the sampling time varied on different sampling days. In particular, many  
 6 whole air samples were collected during O<sub>3</sub> episodes at Tai O. These could also  
 7 induce differences in observed levels among the three sites. At the urban TW site, the  
 8 mean mixing ratios of alkyl nitrates were lower than those measured in urban areas in  
 9 Europe (Worton et al., 2010) and China (Wang et al., 2013). Compared to the average  
 10 values of alkyl nitrates at Tai O, the levels of EtONO<sub>2</sub>, 1-PrONO<sub>2</sub> and 2-BuONO<sub>2</sub>  
 11 were slightly higher and the MeONO<sub>2</sub> and 2-PrONO<sub>2</sub> mixing ratio was lower at TW.

12

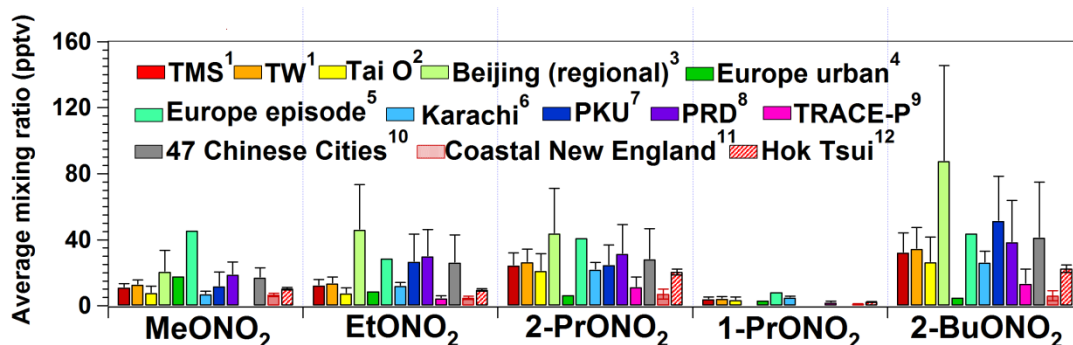
13 Table 1 Descriptive statistics of alkyl nitrates and parent hydrocarbons (pptv) in whole  
 14 air samples collected at TMS and TW during the sampling period.

Species	TMS					TW				
	Mean*	Min.	Max.	10 <sup>th</sup> #	90 <sup>th</sup> #	Mean	Min.	Max.	10 <sup>th</sup> #	90 <sup>th</sup> #
MeONO <sub>2</sub>	10.9±0.4	6.2	21.4	8.1	13.6	12.6±0.5	7.2	26.6	9.2	16.4
EtONO <sub>2</sub>	12.1±0.5	3.2	25.6	7.6	16.5	13.3±0.6	4.0	35.0	8.3	18.1
2-PrONO <sub>2</sub>	24.1±1.1	4.0	51.2	14.8	34.7	26.3±1.2	6.0	49.2	16.2	36.2
1-PrONO <sub>2</sub>	3.8±0.2	0.4	10.6	1.9	5.5	4.0±0.2	0.7	8.1	2.2	6.1
2-BuONO <sub>2</sub>	32.0±1.7	3.1	80.1	18.8	46.6	34.2±1.9	5.1	92.8	20.8	49.2
Methane (ppmv)	2.0±0.1	1.8	2.2	1.9	2.0	2.0±0.1	1.8	2.5	1.9	2.0
Ethane	1908±78	396	3588	1154	2470	2224±90	717	4315	1359	2906
Propane	1101±75	106	4455	569	1749	3551±415	1443	33800	1844	5153
<i>n</i> -Butane	830±91	97	6252	349	1517	4486±482	1372	34700	2168	7633

15 \* Average ± 95% confidence interval

16 # 10<sup>th</sup> and 90<sup>th</sup> percentiles

17



18

1 Figure 2. Comparison of alkyl nitrate mixing ratios in different locations. Data  
 2 collected by UCI before 2008 (PRD and TRACE-P) were adjusted to UCI's new  
 3 calibration scale to permit direct comparison (see text for details about the new  
 4 calibration.

5 <sup>1</sup>. This study, September-November, 2010. <sup>2</sup>. Rural site, August 2001-December 2002 (Simpson et  
 6 al., 2006). <sup>3</sup>. Urban site, 2009-2011 (Wang et al., 2013). <sup>4</sup>. Urban sites, April-May 2004 (Worton et  
 7 a., 2010). <sup>5</sup>. Urban sites, April-May 2004 (Worton et al., 2010). <sup>6</sup>. Coastal site, December  
 8 1998-January 1999 (Barletta et al., 2002). <sup>7</sup>. Urban site, August-September 2011 and December  
 9 2011-January 2012 (Wang et al., 2013). <sup>8</sup>. Regional background sites, September 2009 (Wang et al.,  
 10 2013). <sup>9</sup>. Aircraft measurement, February-April 2001 (Simpson et al., 2003). <sup>10</sup>. Urban sites, July  
 11 2009 (Wang et al., 2013). <sup>11</sup>. Coastal site, January-February and June-August 2002, July-August  
 12 2004 (Russo et al., 2010). <sup>12</sup>. Regional background site, March 2001-April 2002 (unpublished  
 13 data).

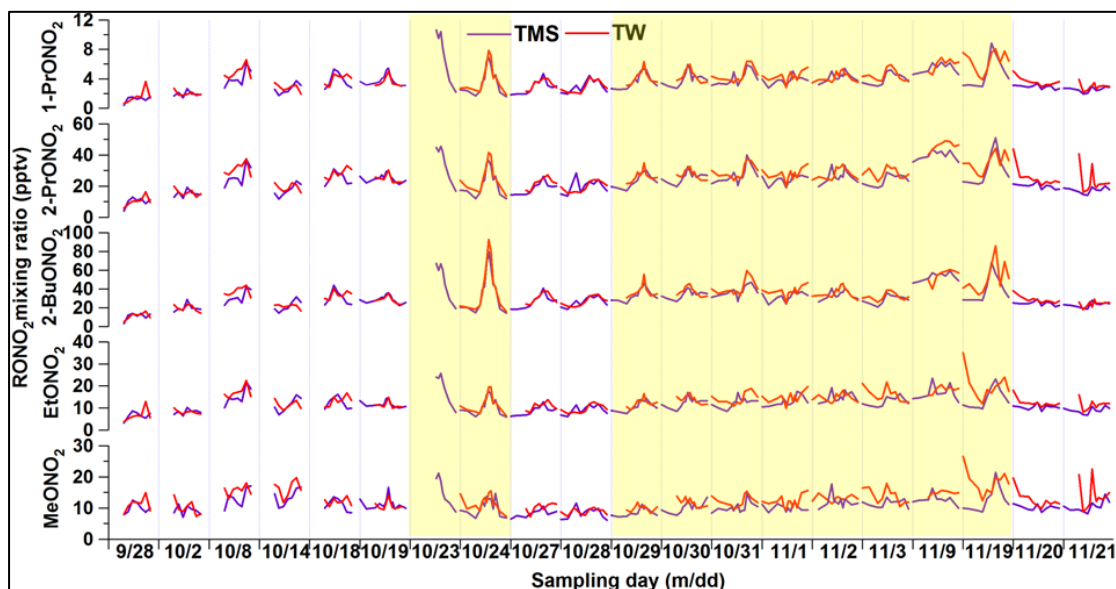
14  
 15  
 16 Table 2 Descriptive statistics of alkyl nitrate (pptv) and parent hydrocarbons (ppbv) in  
 17 whole air samples collected at Tai O between 24 August 2001 and 31 December 2002  
 18 (from Simpson et al., 2006).

Compound	Minimum	Maximum	Median	Mean
MeONO <sub>2</sub>	5.5	52.2	13.4	15.9
EtONO <sub>2</sub>	2.7	34.3	12.1	13.1
1-PrONO <sub>2</sub>	0.2	14.5	3.5	3.9
2-PrONO <sub>2</sub>	2.4	65.9	24.5	32.6
2-BuONO <sub>2</sub>	0.8	89.8	27.4	30.7
Methane (ppmv)	1.75	3.70	1.96	2.05
Ethane (ppbv)	0.38	5.05	2.14	2.12
Propane (ppbv)	0.006	13.0	1.54	2.05
<i>n</i> -Butane (ppbv)	0.006	12.8	0.95	1.64

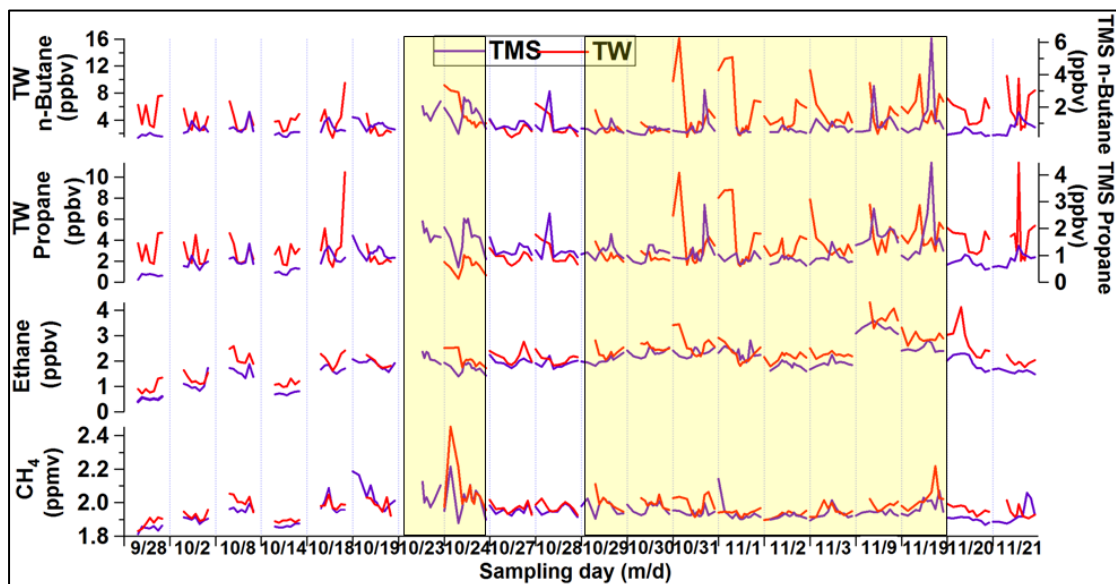
19  
 20 Table S2 and Figure S2 in the supplementary information summarize the  
 21 synoptic weather conditions and the corresponding variations of O<sub>3</sub> and alkyl nitrates  
 22 on O<sub>3</sub> episode and non-O<sub>3</sub> episode days at both sites. In general, meteorological  
 23 conditions including temperatures, winds and solar radiation significantly influenced  
 24 the levels of air pollutants (Table S2). High mixing ratios of O<sub>3</sub> and alkyl nitrates were  
 25 usually associated with meteorological conditions with high-pressure system and/or  
 26 stable conditions, such as high temperatures, intense solar radiation and low wind  
 27 speeds. Figure 3 shows the time series of C<sub>1</sub>-C<sub>4</sub> alkyl nitrates on O<sub>3</sub> episode and  
 28 non-O<sub>3</sub> episode days at both sites, while Figure 4 presents the temporal variations of

1 their parent hydrocarbons accordingly. Although the ranges of alkyl nitrate mixing  
2 ratios were similar and maximum values were observed in the afternoon, the  
3 day-to-day variations of individual alkyl nitrates differed during the sampling period  
4 at both sites. The maximum values were comparable and the diurnal patterns tracked  
5 each other for the C<sub>3</sub>-C<sub>4</sub> alkyl nitrates at TMS and TW, especially on the days (24  
6 October to 3 November, 9 and 19 November) with relatively higher O<sub>3</sub> mixing ratios  
7 ( $p < 0.05$ ). The average daytime O<sub>3</sub> mixing ratios (0700-1800) on the high O<sub>3</sub> days  
8 were  $77 \pm 3$  and  $38 \pm 3$  ppbv at TMS and TW, respectively, compared to  $58 \pm 3$  and  
9  $23 \pm 3$  ppbv, on the non-O<sub>3</sub> episode days. Typically, the average daytime levels of  
10 2-PrONO<sub>2</sub>, 1-PrONO<sub>2</sub> and 2-BuONO<sub>2</sub> on **high O<sub>3</sub> days** at TMS were  $27 \pm 1$  (TW:  $28$   
11  $\pm 1$ ),  $4.5 \pm 0.3$  ( $4.4 \pm 0.2$ ) and  $37 \pm 2$  ( $39 \pm 3$ ) pptv, respectively, higher than those on  
12 non-O<sub>3</sub> episode days ( $p < 0.05$ ), implying that secondary formation of alkyl nitrates  
13 might be more prominent on O<sub>3</sub> episode days. Coincident with the high C<sub>3</sub>-C<sub>4</sub> alkyl  
14 nitrates during high O<sub>3</sub> days, their parent hydrocarbons, *i.e.*, propane (0.56-4.46 and  
15 1.55-10.4 ppbv for TMS and TW, respectively) and *n*-butane (0.28-6.25 and 1.47-16.1  
16 ppbv, respectively) also showed elevated mixing ratios (Figure 4), further suggesting  
17 an important source of C<sub>3</sub>-C<sub>4</sub> alkyl nitrates which was photo-oxidation of the parent  
18 hydrocarbons. For the C<sub>1</sub>-C<sub>2</sub> alkyl nitrates, the temporal patterns of MeONO<sub>2</sub> and  
19 EtONO<sub>2</sub> were different at the two sites, especially on high-level O<sub>3</sub> days. The peaks of  
20 MeONO<sub>2</sub> and EtONO<sub>2</sub> were usually observed between 11 a.m. and 4 p.m. at TMS,  
21 except for 14 and 28 October, 1-2, 9, 20-21 November. The peaks of C<sub>1</sub>-C<sub>2</sub> alkyl  
22 nitrates corresponded to the high levels of methane and ethane observed at 11 a.m. to  
23 5 p.m., likely resulted from regional transport (Guo et al., 2009; Jiang et al., 2010)  
24 and/or mesoscale circulations (Gao et al., 2005; Wang et al., 2006) (Section 3.2.3). At  
25 TW, however, besides the maximum concentrations observed in the afternoon, high  
26 levels of MeONO<sub>2</sub> and EtONO<sub>2</sub> were observed from midnight to early morning on 13  
27 out of the 19 sampling days (*i.e.*, 2, 8, 14, 24, 28, 30-31 October, 1-3, 19-21  
28 November), when the prevailing winds switched to the southeast direction, implying  
29 that the high levels of MeONO<sub>2</sub> and EtONO<sub>2</sub> are likely related to marine emissions  
30 and aged continental plumes which were re-circulated from the South China Sea to

1 the coastal urban site at night. Indeed, this speculation was supported by the source  
 2 apportionment results at TW, which confirmed that the high MeONO<sub>2</sub> and EtONO<sub>2</sub>  
 3 levels from midnight to early morning on the above sampling days were related to  
 4 oceanic emissions (see Section 3.2.2 for details).



5  
 6 Figure 3. Time series of MeONO<sub>2</sub>, EtONO<sub>2</sub>, 1-PrONO<sub>2</sub>, 2-PrONO<sub>2</sub> and 2-BuONO<sub>2</sub>  
 7 measured at TMS (purple) and TW (red) in 2010. The yellow shading highlights the  
 8 O<sub>3</sub> episode days.



10  
 11 Figure 4. Time series of the parent hydrocarbons of alkyl nitrates at TMS and TW.  
 12 The yellow shading highlights the O<sub>3</sub> episode days.

13  
 14 Although the levels of the parent hydrocarbons were lower at TMS, similar

1 values of alkyl nitrates were observed at both sites, regardless of the elevation,  
 2 suggesting the contributions of different sources and/or the influences of different air  
 3 masses. Hence, the source apportionments of alkyl nitrates, contributions of reaction  
 4 pathways for the secondary formation of alkyl nitrates, and the relationship between  
 5 O<sub>3</sub> and alkyl nitrates were analyzed in the following sections.

## 6 **3.2. Sources of alkyl nitrates**

### 7 **3.2.1. Photochemical evolution of alkyl nitrates**

8 As photochemical oxidation of parent hydrocarbons is an important source of  
 9 alkyl nitrates, it is valuable to study the photochemical evolution of alkyl nitrates. To  
 10 do so, the relationships of alkyl nitrates with their parent hydrocarbons at the two sites  
 11 were further examined using a simplified sequential reaction model developed by  
 12 Bertman et al. (1995) (Equation 1), based on the assumptions that: (i) the hydrogen  
 13 abstraction reaction from the parent hydrocarbon was the rate-limiting step for  
 14 photochemical production of alkyl nitrates, and (ii) the reaction environment was  
 15 NO<sub>x</sub>-rich, making the reaction with NO being the dominant pathway for the removal  
 16 of RO<sub>2</sub> radicals (Russo et al., 2010). In this study, the average mixing ratios of NO<sub>x</sub> at  
 17 TMS and TW were 10.7 ± 0.3 and 56.3 ± 1.6 ppbv, respectively, indicating that the  
 18 environment was NO<sub>x</sub>-rich (> 0.1 ppbv, Roberts et al., 1998). Hence, reaction with  
 19 NO was the main pathway for the removal of RO<sub>2</sub> radicals at the two sites. In addition,  
 20 the results of PBM-MCM model simulation confirmed that the hydrogen abstraction  
 21 reaction from the parent hydrocarbon, namely the reaction of hydrocarbon with OH  
 22 radical, was indeed the rate-limiting step for photochemical production of alkyl  
 23 nitrates at both sites (Lyu et al., 2015).

$$24 \left| \frac{RONO_2}{RH} = \frac{\beta k_A}{k_B - k_A} (1 - e^{(k_A - k_B)t}) + \frac{[RONO_2]_0}{[RH]_0} e^{(k_A - k_B)t} \quad (\text{Equation 1}) \right.$$

25 where  $\beta = \alpha_1 \alpha_2$ ,  $k_A$  is the production rate for the formation of alkyl nitrates  
 26 through the oxidation of hydrocarbons, RH ( $k_A = k_1[\text{OH}]$ ), while  $k_B$  is the destruction  
 27 rate for alkyl nitrates through photolysis and the reaction with OH ( $k_B = k_5[\text{OH}] +$   
 28  $J_{\text{RONO}_2}$ ).  $[RONO_2]_0$  and  $[RH]_0$  are the initial concentrations of alkyl nitrates and the  
 29 parent hydrocarbons before photochemical processing, respectively;  $[\text{OH}]$  is the

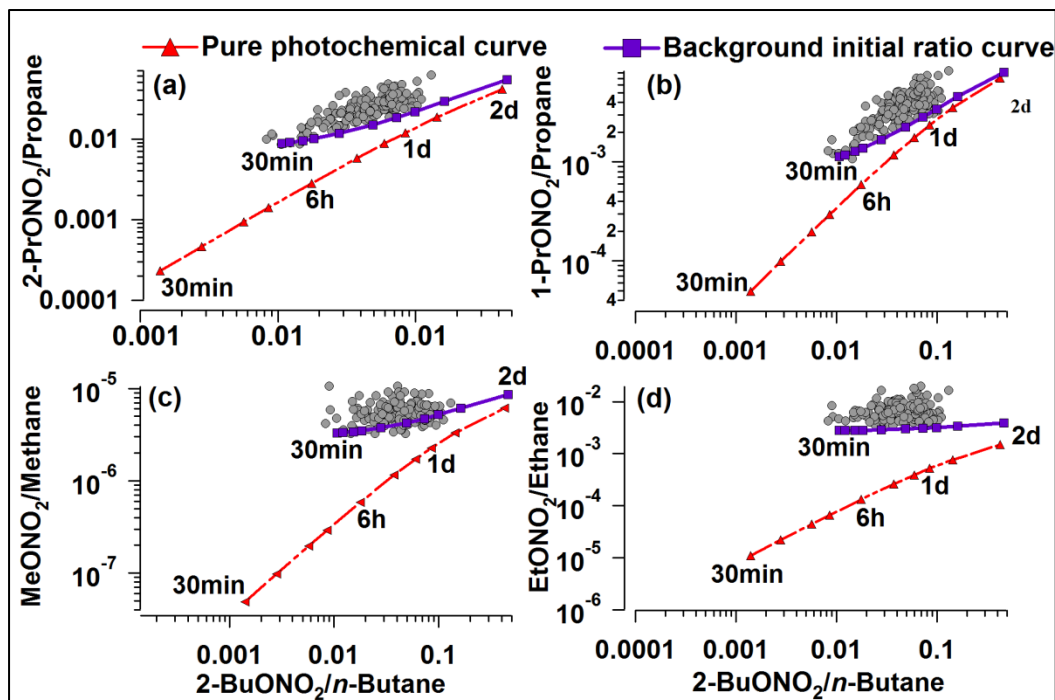
1 diurnal average concentration of the OH radical. The relationships of alkyl nitrates  
2 with their parent hydrocarbons derived from the preceding equation are comparatively  
3 independent of the variations of OH and photolysis rates of alkyl nitrates (Roberts et  
4 al., 1998; Wang et al., 2013). If the initial concentrations of alkyl nitrates and RH are  
5 zero, Equation 1 can be expressed as follows (Equation 2):

$$6 \left| \frac{RONO_2}{RH} = \frac{\beta k_A}{k_B - k_A} (1 - e^{(k_A - k_B)t}) \quad \text{(Equation 2)} \right.$$

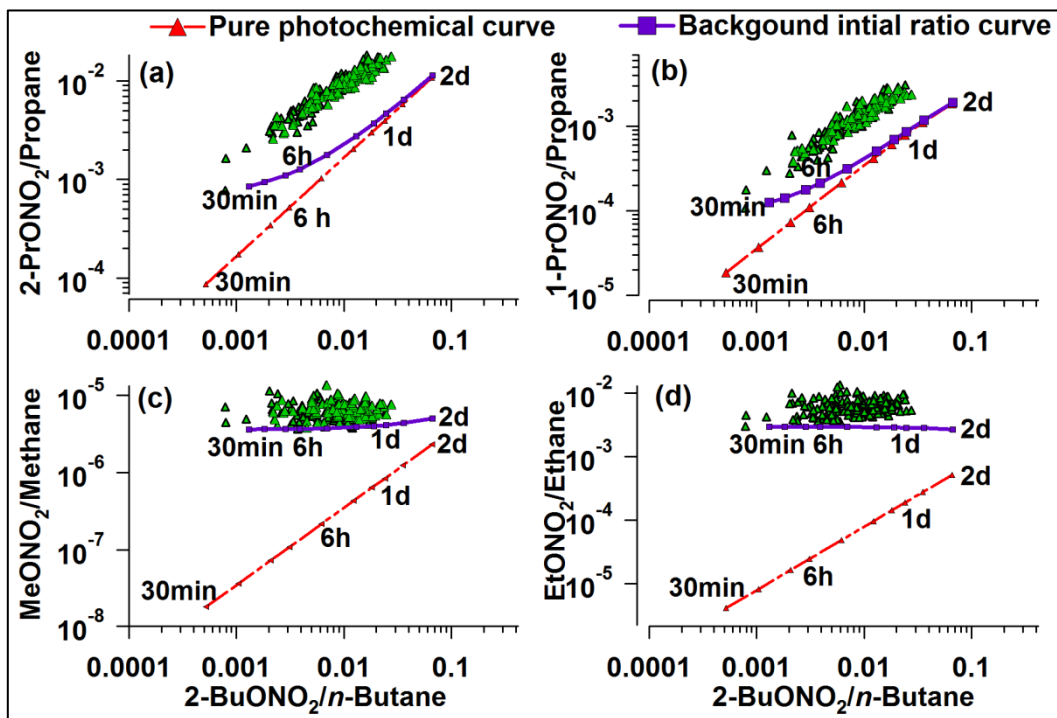
7 The relationships between alkyl nitrates and RH are obtained by plotting the  
8 measured ratios of  $RONO_2/RH$  to a specific ratio, 2-BuONO<sub>2</sub>/*n*-butane. The  
9 2-BuONO<sub>2</sub>/*n*-butane ratio has been widely used in the analysis of alkyl nitrates because  
10 *n*-butane is typically one of the most abundant hydrocarbons and 2-BuONO<sub>2</sub> is the  
11 dominant alkyl nitrate (Roberts et al., 1998; Wang et al., 2013; Worton et al., 2010).  
12 Although some studies have investigated the relationships between alkyl nitrates and  
13 their parent hydrocarbons using zero initial values of alkyl nitrates, more recent  
14 studies have used non-zero initial values of alkyl nitrates to evaluate the influence of  
15 background levels on the photochemical evolution of alkyl nitrates (Reeves et al.,  
16 2007; Russo et al., 2010; Wang et al., 2013). Therefore, in addition to zero initial  
17 ratios, non-zero initial ratios of  $RONO_2/RH$ , equal to the lowest values from 0000 to  
18 0700 measured at TMS and TW, respectively, as suggested by Wang et al. (2013),  
19 were used to investigate the relationships between alkyl nitrates and their parent  
20 hydrocarbons in this study. The diurnal average OH mixing ratios were simulated  
21 using the PBM-MCM (Lyu et al., 2016). By providing the values of photochemical  
22 processing time (*t*), the predicted ratios of  $RONO_2/RH$  were calculated since other  
23 parameters, *i.e.*,  $k_A$ ,  $k_B$ ,  $\alpha_1$ ,  $\alpha_2$  and  $J_{RONO_2}$  were obtained from literature (Clemitshaw et  
24 al., 1997; Simpson et al., 2003; Worton et al., 2010; Wang et al., 2013). In this study,  
25 the given photochemical processing time ranged from 30 min to 2 days. The curves  
26 generated with zero initial values were the pure photochemical (PP) curves for the  
27 evolution of alkyl nitrates, and the curves with non-zero values, defined as  
28 background initial ratio (BIR) curves, were generated by assuming that both  
29 photochemical formation and background levels contributed to the distribution of



1 alkyl nitrates (Russo et al., 2010; Wang et al., 2013). Consistent with previous studies  
 2 (Russo et al., 2010; Wang et al., 2013), the shapes of the BIR curves were different  
 3 from those of PP curves. The BIR curves of C<sub>1</sub>-C<sub>3</sub> alkyl nitrates at both sites were  
 4 positioned above their PP curves at shorter processing time ( $t < 1$  d) and converged  
 5 towards the PP curves at longer processing times ( $t = 1.5$ -2 d) (Figure 5), resulting  
 6 from the decreased influence of the parameter  $\frac{[RONO_2]_0}{[RH]_0} e^{(k_A - k_B)t}$  on the difference  
 7 between the two curves as the photochemical age increased (Wang et al., 2013). This  
 8 feature was more pronounced for C<sub>3</sub>-C<sub>4</sub> alkyl nitrates at TW (Figure 6) because of the  
 9 lower values of  $[RONO_2]_0/[RH]_0$  resulting from the high mixing ratios of propane and  
 10 *n*-butane (Ling and Guo, 2014). Figure 5 presents the relationships of C<sub>1</sub>-C<sub>3</sub>  
 11  $RONO_2/RH$  to 2-BuONO<sub>2</sub>/*n*-butane at TMS. The red dashed curves are pure  
 12 photochemical curves, while the blue solid curves are BIR curves with the lowest  
 13 ratios of  $RONO_2/RH$  from 0000 to 0700 LT as the background initial ratio. Similarly,  
 14 Figure 6 shows the relationships of C<sub>1</sub>-C<sub>3</sub>  $RONO_2/RH$  to 2-BuONO<sub>2</sub>/*n*-butane at TW.



15  
 16 Figure 5. Relationships of C<sub>1</sub>-C<sub>3</sub>  $RONO_2/RH$  with 2-BuONO<sub>2</sub>/*n*-butane at TMS. The  
 17 red dashed curves were obtained based on zero initial concentrations of RH and alkyl  
 18 nitrates (pure photochemical curves, PP), while the blue solid curves were obtained  
 19 based on non-zero initial levels (background initial ratio curves, BIR), with the lowest  
 20 ratios of  $RONO_2/RH$  from 0000 to 0700 LT.



1

2 Figure 6. Relationships of C<sub>1</sub>-C<sub>3</sub> RONO<sub>2</sub>/RH with 2-BuONO<sub>2</sub>/*n*-butane at TW. The  
 3 red dashed curves were obtained based on zero initial concentrations of RH and alkyl  
 4 nitrates (pure photochemical curves, PP), while the blue solid curves were obtained  
 5 based on non-zero initial levels (background initial ratio curves, BIR), with the lowest  
 6 ratios of RONO<sub>2</sub>/RH from 0000 to 0700 LT.

7

8 At TMS, the measured ratios of MeONO<sub>2</sub>/methane and EtONO<sub>2</sub>/ethane to  
 9 2-BuONO<sub>2</sub>/*n*-butane were much higher than the ratios in the PP curves (Figure 5c &  
 10 d), with the observed ratios larger than their theoretical ratios by factors of 5-25. As  
 11 expected, the observed trends approached the PP curves at a longer processing time,  
 12 suggesting that the measured ratios of C<sub>1</sub>-C<sub>2</sub> RONO<sub>2</sub>/RH to 2-BuONO<sub>2</sub>/*n*-butane were  
 13 influenced by aged air masses resulting from their relatively long atmospheric  
 14 lifetimes and the slow photochemical reaction rates of methane and ethane (Worton et  
 15 al., 2010; Russo et al., 2010). However, the difference between the measured ratios  
 16 and the predicted ratios of C<sub>1</sub>-C<sub>2</sub> RONO<sub>2</sub>/RH to 2-BuONO<sub>2</sub>/*n*-butane in BIR curves  
 17 was comparatively smaller, further confirming that there were other sources  
 18 contributing to ambient C<sub>1</sub>-C<sub>2</sub> alkyl nitrates besides photochemical formation,  
 19 including the background levels of C<sub>1</sub>-C<sub>2</sub> alkyl nitrates and their parent hydrocarbons  
 20 (direct measurements of RH in Table 1) (Wang et al., 2013). For example, the average

1 MeONO<sub>2</sub> and EtONO<sub>2</sub> mixing ratios at Hok Tsui, a PRD regional background site,  
2 were  $10.4 \pm 0.7$  and  $9.6 \pm 0.7$  pptv (unpublished data, 2001-2002), respectively.

3 Regarding the C<sub>3</sub> alkyl nitrates, the measured ratios of 1- and 2-PrONO<sub>2</sub>/propane  
4 to 2-BuONO<sub>2</sub>/*n*-butane were closer to the ratios of the BIR curve than those of the PP  
5 curve at TMS, further indicating the influence of background C<sub>3</sub> alkyl nitrates and  
6 their parent hydrocarbons. However, the evolution of the measured ratios of C<sub>3</sub>  
7 RONO<sub>2</sub>/RH to 2-BuONO<sub>2</sub>/*n*-butane agreed well with the predicted ratios of BIR and PP  
8 curves at TMS, indicating that secondary formation from propane oxidation  
9 contributed significantly to the ambient C<sub>3</sub> alkyl nitrates, including the background C<sub>3</sub>  
10 alkyl nitrates. Consistent with previous studies, the slopes of the observed ratios of C<sub>3</sub>  
11 RONO<sub>2</sub>/RH to 2-BuONO<sub>2</sub>/*n*-butane were different from those in the PP and BIR  
12 curves (Russo et al., 2010; Wang et al., 2013). For example, the slopes of the observed  
13 ratios of 1- and 2-PrONO<sub>2</sub>/propane to 2-BuONO<sub>2</sub>/*n*-butane were  $0.04 \pm 0.01$  and  $0.26$   
14  $\pm 0.02$ , respectively, while the slopes for the BIR curves were  $0.02 \pm 0.01$  (PP curve:  
15  $0.02 \pm 0.01$ ) and  $0.12 \pm 0.01$  ( $0.10 \pm 0.01$ ), respectively. This was reasonable as the  
16 difference in the number of samples and distribution of data between the observed  
17 ratios and the ratios of PP and BIR curves, particularly when the observed ratios were  
18 higher than the theoretical ones because of significant influence of the background  
19 levels of alkyl nitrates and RH (Russo et al., 2010; Wang et al., 2013). Therefore, to  
20 further investigate the influence of secondary formation and background mixing ratios  
21 on C<sub>3</sub> alkyl nitrates at TMS, the ratio of 1-/2-PrONO<sub>2</sub> was examined. Previous studies  
22 reported that the theoretical ratio of 1-/2-PrONO<sub>2</sub> was the ratio between the yield for  
23 1-PrONO<sub>2</sub> and 2-PrONO<sub>2</sub> formation, which was equal to the ratio of  
24  $\beta_{1\text{-PrONO}_2}/\beta_{2\text{-PrONO}_2}$  (0.21) (Simpson et al., 2003; Wang et al., 2013). If photochemical  
25 production was the dominant source of 1-PrONO<sub>2</sub> and 2-PrONO<sub>2</sub>, the observed ratios  
26 should be close to the theoretical ones. Indeed, the slope of 1-PrONO<sub>2</sub> and 2-PrONO<sub>2</sub>  
27 at TMS was 0.19 ( $R^2 = 0.86$ ,  $p < 0.05$ ), close to the theoretical ratio (0.21), confirming  
28 that photochemical production from propane, including in-situ photochemical  
29 production and transport of photochemically-formed C<sub>3</sub> alkyl nitrates in urban areas  
30 and/or during transit from urban areas to TMS, was the dominant source of ambient

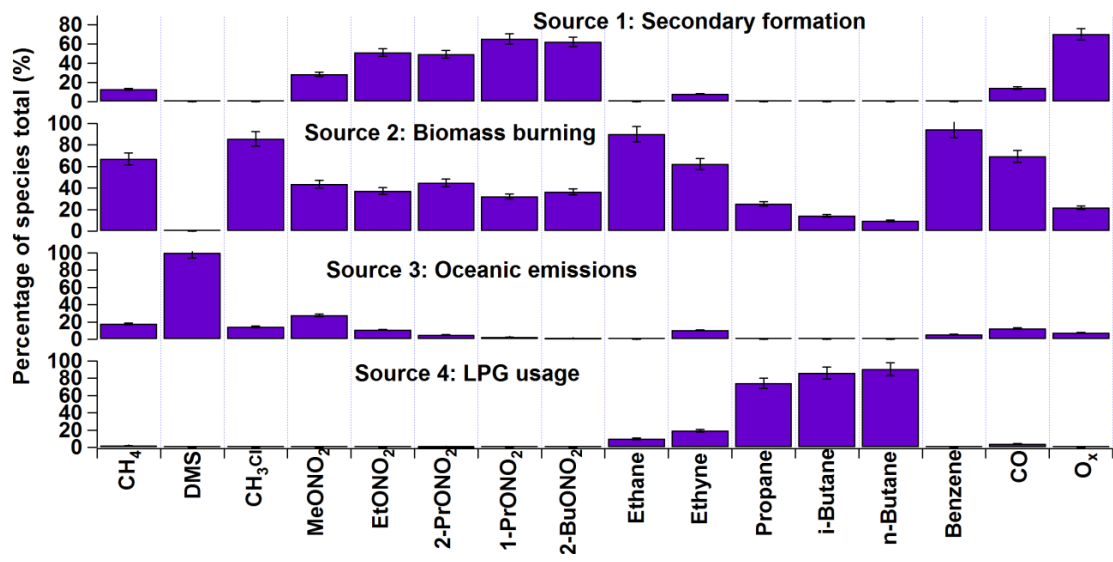
1 C<sub>3</sub> alkyl nitrates.

2 At TW, the comparison between the observed ratios of C<sub>1</sub>-C<sub>2</sub> RONO<sub>2</sub>/RH to  
3 2-BuONO<sub>2</sub>/*n*-butane and the ratios from the PP and BIR curves was consistent with  
4 that at TMS. However, in terms of C<sub>3</sub> alkyl nitrates, although the evolution of the  
5 measured ratios of C<sub>3</sub> RONO<sub>2</sub>/RH to 2-BuONO<sub>2</sub>/*n*-butane followed the trends of the  
6 ratios in the PP and BIR curves, the measured ratios of C<sub>3</sub> RONO<sub>2</sub>/RH to  
7 2-BuONO<sub>2</sub>/*n*-butane at TW were further away from the PP/BIR curves, about 2-3  
8 times the ratios in the PP and BIR curves, implying additional sources of C<sub>3</sub> alkyl  
9 nitrates (Wang et al., 2013) (details in Section 3.2.2). High emissions of propane  
10 provided sufficient precursors of C<sub>3</sub> alkyl nitrates, and the lifetimes of 1-PrONO<sub>2</sub> and  
11 2-PrONO<sub>2</sub> were long enough to sustain relatively high levels at TW. To further  
12 investigate the influence of additional sources on the distributions of C<sub>3</sub> alkyl nitrates  
13 at TW, equation 1 was used to fit the measured ratios of 1- and 2-PrONO<sub>2</sub>/propane to  
14 calculate the yield of C<sub>3</sub> alkyl nitrates ( $\beta$ ). The average yields of 1- and 2-PrONO<sub>2</sub>  
15 were  $0.032 \pm 0.004$  and  $0.22 \pm 0.02$ , respectively, higher than the laboratory kinetic  
16 values by factors of 4–9 (Kwok and Atkinson, 1995). This confirms the presence of  
17 additional emissions of C<sub>3</sub> alkyl nitrates at TW, including locally-emitted C<sub>3</sub> alkyl  
18 nitrates and/or secondary formation other than the production pathway from propane  
19 to proxyl radical and PrONO<sub>2</sub> (Reeves et al., 2007; Worton et al., 2010). The slope of  
20 1-PrONO<sub>2</sub> to 2-PrONO<sub>2</sub> at TW was 0.15 ( $R^2 = 0.80$ ,  $p < 0.05$ ), lower than the  
21 theoretical ratio of 0.21, further demonstrating the influence of other significant  
22 sources on ambient mixing ratios of C<sub>3</sub> alkyl nitrates at TW.

### 23 3.2.2. Source apportionment of alkyl nitrates

24 Figure 7 presents the explained variations of species (as a percentage of the  
25 species total) in the identified sources extracted by the PMF model. The **standard error**  
26 **in Figure 7 was obtained from a bootstrap analysis of the PMF model simulation. The**  
27 **source profiles of the alkyl nitrates and their parent hydrocarbons were altered**  
28 **resulting from photochemical transformation during transport to the TMS site.**  
29 Therefore, only the data collected at the urban site were used for source  
30 apportionments of alkyl nitrates.

1 High concentrations of O<sub>x</sub> and alkyl nitrates were found in the first factor at both  
 2 sites, implying that this factor was associated with secondary formation. In addition,  
 3 certain amounts of combustion species, such as ethane, ethyne, propane, *i/n*-butanes,  
 4 benzene and CO were present in this factor. It is not surprising that O<sub>x</sub> correlated with  
 5 the aforementioned species given that O<sub>3</sub> is a secondary pollutant formed from  
 6 photochemical oxidation of RH (Ling and Guo, 2014). The second factor was  
 7 distinguished by a significant presence of methyl chloride, ethene, ethyne and  
 8 benzene along with certain amounts of methane, propane and *i/n*-butane. It is well  
 9 established that methyl chloride, ethyne and benzene are typical tracers for biomass  
 10 burning/biofuel combustion (Barletta et al., 2009; Guo et al., 2011). As biofuel was  
 11 not in widespread use in Hong Kong (HKCSD, 2010), this factor was identified as  
 12 biomass burning. The third factor was identified as oceanic emissions, as the tracer  
 13 DMS had an exclusively high percentage in this source at both sites (Blake et al.,  
 14 2003; Marandino et al., 2013). The last factor was dominated by high percentages of  
 15 propane and *i/n*-butanes, typical tracers of liquefied petroleum gas (LPG). Therefore,  
 16 this factor was identified as LPG usage.



17  
 18 Figure 7. Explained variations of species in the identified sources extracted by the  
 19 PMF model for TW.

20 As mentioned earlier, regional transport and mesoscale circulation had a  
 21 significant influence on the distribution of air pollutants at TMS and TW (Guo et al.,  
 22 2012, 2013a). By using the Weather Research and Forecasting (WRF) model, air

1 masses affected by mesoscale circulation were distinguished from those affected by  
2 regional transport (Guo et al., 2013a). Nine sampling days during the entire sampling  
3 period (24, 29-31 October, 1-3, 9 and 19 November) were identified to be affected by  
4 mountain-valley breezes (they were also O<sub>3</sub> episode days). Hence, we divided the  
5 sampling period into two categories - “meso” and “non-meso” scenarios for source  
6 apportionment analysis. The “meso” scenario included the nine O<sub>3</sub> episode days with  
7 apparent mesoscale circulation, while the “non-meso” scenario covered the rest of the  
8 sampling days.

9 By summing up the mass of the alkyl nitrates in each source category, the overall  
10 mixing ratios in each source were obtained and the contribution of each individual  
11 source to alkyl nitrates at both sites was calculated. Figures 8 and 9 present the source  
12 contributions to individual alkyl nitrates for the “meso” and “non-meso” scenarios in  
13 percentage and in mixing ratio at TW, respectively. The mixing ratios of total alkyl  
14 nitrates (*i.e.*,  $\sum \text{RONO}_2 = \text{MeONO}_2 + \text{EtONO}_2 + 1\text{-PrONO}_2 + 2\text{-PrONO}_2 +$   
15  $2\text{-BuONO}_2$ ) were higher in the “meso” scenario than those in “non-meso” scenario ( $p$   
16  $< 0.05$ ), with the average value of  $100.9 \pm 7.5$  pptv for total alkyl nitrates in the “meso”  
17 scenario, about 1.4 times those in the “non-meso” scenario. It was found that in the  
18 “meso” scenario, secondary formation was the most significant contributor to the total  
19 alkyl nitrate mixing ratios, with an average percentage of  $60 \pm 2\%$  or absolute mixing  
20 ratio of  $60.2 \pm 1.2$  pptv, followed by biomass burning ( $34 \pm 1\%$  or  $35.1 \pm 0.4$  pptv)  
21 and oceanic emissions ( $6 \pm 1\%$  or  $5.62 \pm 0.06$  pptv). For the “non-meso” scenario, the  
22 contributions of biomass burning ( $46 \pm 2\%$  or  $34.2 \pm 0.7$  pptv) and secondary  
23 formation ( $44 \pm 2\%$  or  $32.9 \pm 0.7$  pptv) were comparable, and the oceanic emissions  
24 contributed  $10 \pm 1\%$  or  $7.0 \pm 0.07$  pptv to the total alkyl nitrates. The higher  
25 contribution of secondary formation in the “meso” scenario at TW was mainly  
26 | associated with higher degree of photochemical reactions. Indeed, the PBM-MCM  
27 model simulation indicated that the average concentration of HO<sub>x</sub> (HO<sub>x</sub> = OH + HO<sub>2</sub>)  
28 during daytime hours (0700-1800 LT) in the “meso” scenario was  $(2.5 \pm 0.7) \times 10^7$   
29 molecule/cm<sup>3</sup>, about twice that of the “non-meso” scenario.

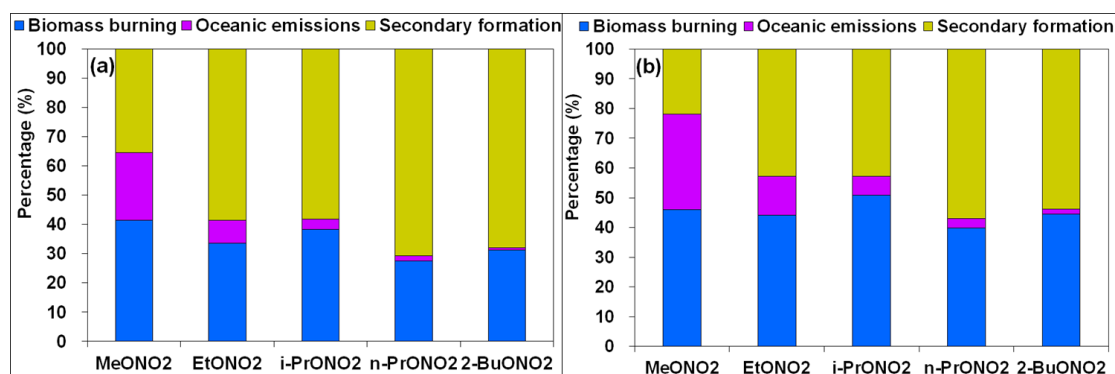


Figure 8. Source contributions to individual alkyl nitrates in (a) “meso” and (b) “non-meso” scenarios at TW (in percentage).

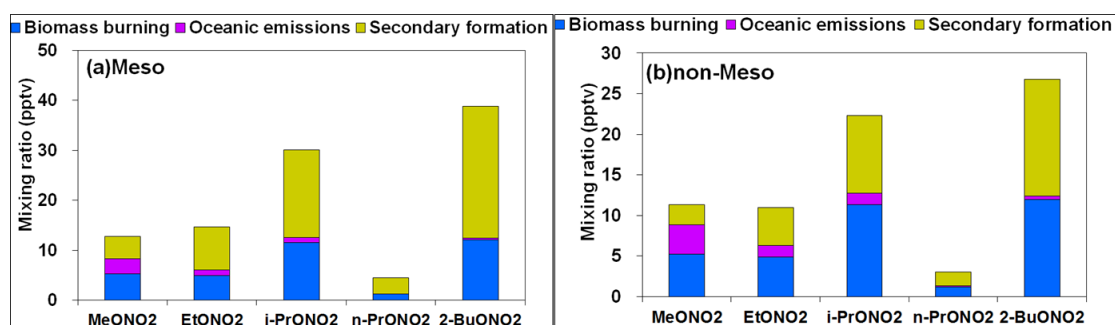
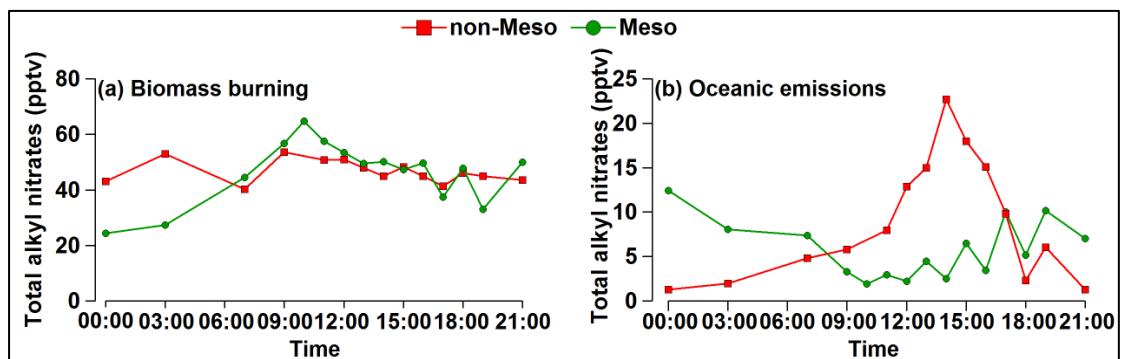


Figure 9. Source contributions to individual alkyl nitrates in (a) “meso” and (b) “non-meso” scenarios at TW (in summed mixing ratio).

In addition, although the percentage contribution of biomass burning was higher in the “non-meso” scenario, the absolute mixing ratios of biomass burning were comparable in the two scenarios. Figure 10 shows the diurnal patterns of  $\Sigma$ RONO<sub>2</sub> from biomass burning and oceanic emissions in “meso” and “non-meso” scenarios at TW. The contribution of biomass burning in the “meso” scenario was likely attributable to local emissions, including the cooking/heating activities in the small villages nearby and the frequent barbecue activities at the base of the mountain (Guo et al., 2013a, b), as well as the forest fires observed in the mountainous areas (AFCD, 2015). The regular cooking/heating activities from 0700 to 1400 LT in many dim sum restaurants in the village likely resulted in the increased levels of biomass burning in the morning until noon. In contrast, the diurnal pattern in “non-meso” scenario was weak and the maximum values were not statistically different from the minimum values. The difference of the average mixing ratio of  $\Sigma$ RONO<sub>2</sub> between daytime and nighttime hours was only 1 pptv for biomass burning. The weak diurnal variations in

1 the “non-meso” scenario suggests that the contribution of fresh biomass burning  
 2 emissions was insignificant, revealing the influence of regional transport from the  
 3 PRD region. This speculation was confirmed by the analysis of 12-h backward  
 4 trajectories, which showed that air masses in the “non-meso” scenario were mainly  
 5 from the inland PRD region (not shown). It is noteworthy that although air masses  
 6 were more aged in the “non-meso” scenario, the levels of alkyl nitrates were  
 7 comparable to those in the “meso” scenario, highlighting the strong emissions of  
 8 biomass burning in the PRD region (Yuan et al., 2010).

9 For the oceanic emissions, a minimum mixing ratio during daytime hours was  
 10 found for  $\Sigma \text{RONO}_2$  in the “meso” scenario, while a broad peak was present during  
 11 daytime hours in the “non-meso” scenario. The daytime minimum mixing ratio in the  
 12 “meso” scenario at TW was related to uplifted valley breezes that brought alkyl  
 13 nitrates away from TW to TMS, while the higher nighttime values were probably  
 14 owing to marine emissions and aged continental plumes which were re-circulated  
 15 from the South China Sea to the coastal urban site at night. In contrast, the broad  
 16 daytime peak in the “non-meso” scenario was likely associated with higher daytime  
 17 temperature and solar radiation, leading to higher oceanic emissions that were  
 18 transported from eastern China and southern China coastal regions to the TW site.



19  
 20 Figure 10. Diurnal patterns of (a) biomass burning and (b) oceanic emissions for  
 21 “meso” and “non-meso” scenarios at TW.  
 22

23 Moreover, the contributions of oceanic emissions to  $C_1$ - $C_2$  alkyl nitrates were  
 24 higher than  $C_3$ - $C_4$  alkyl nitrates, with average percentages of 23% and 32% for the  
 25 “meso” and “non-meso” scenarios (Figures 8 and 9), suggesting the importance of  
 26 oceanic emissions to  $C_1$ - $C_2$  alkyl nitrates, consistent with the results of previous work



1 | (Simpson et al., 2003). The C<sub>3</sub>-C<sub>4</sub> alkyl nitrates were dominated by the secondary  
2 | formation in the “meso” scenario (58-71%), while the contributions of biomass  
3 | burning and secondary formation to C<sub>3</sub>-C<sub>4</sub> alkyl nitrates were comparable in the  
4 | “non-meso” scenario.

### 5 | 6 | **3.2.3. Contributions of mesoscale circulation, in-situ formation and regional** 7 | **transport to alkyl nitrates at TMS**

8 | Valley breezes transported freshly-emitted parent hydrocarbons and alkyl nitrates  
9 | from the urban areas at the base of the mountain (TW) to the mountain summit (TMS)  
10 | during daytime hours, redistributing the ambient levels of alkyl nitrates at TMS (Guo  
11 | et al., 2013a; Lam et al., 2013). Except for MeONO<sub>2</sub>, which had comparable levels in  
12 | both “meso” and “non-meso” scenarios, the mixing ratios of daytime C<sub>2</sub>-C<sub>4</sub> alkyl  
13 | nitrates were all higher in “meso” scenario than those in “non-meso” scenario ( $p <$   
14 |  $0.05$ ), with the average values of  $14.21 \pm 0.79$ ,  $28.73 \pm 1.70$ ,  $4.67 \pm 0.29$  and  $40.21 \pm 2.79$   
15 | pptv for EtONO<sub>2</sub>, *i*-PrONO<sub>2</sub>, *n*-PrONO<sub>2</sub> and 2-BuONO<sub>2</sub>, respectively. To quantify the  
16 | influence of mesoscale circulation on the mixing ratios of alkyl nitrates at TMS, a  
17 | moving box model coupled with master chemical mechanism (Mbox) was applied to  
18 | the data collected on the days influenced by mesoscale circulation (*i.e.*, “meso”  
19 | scenario) (Guo et al., 2013a). The model was developed based on an idealized  
20 | trajectory movement between TMS and TW sites, with air pollutants transported from  
21 | TW to TMS through the valley breeze during daytime hours (0800-1700 LT) when  
22 | photochemical formation of alkyl nitrates was occurring, contributing to their ambient  
23 | levels at TMS. As such, the model was only constrained with the observed daytime  
24 | data at TW. On the other hand, the night-time downslope flow occurred because of the  
25 | mountain breeze after sunset until the next morning, and TMS was set as the center of  
26 | the box model, which was constrained by the data collected at TMS only for that  
27 | period (Lam et al., 2013).

28 | Table 3 presents the average concentrations of C<sub>1</sub>-C<sub>4</sub> alkyl nitrates simulated by  
29 | the Mbox model at TMS, *i.e.*, the values under the “meso” scenario. It should be  
30 | noted that the comparison was only made for daytime alkyl nitrates (0800-1700LT),  
31 | when the valley breeze occurred. The average mixing ratios of MeONO<sub>2</sub>, EtONO<sub>2</sub>,

1 1-PrONO<sub>2</sub>, 2-PrONO<sub>2</sub> and 2-ButONO<sub>2</sub> at daytime hours estimated using the Mbox  
2 model were  $9.97 \pm 0.85$ ,  $7.38 \pm 0.44$ ,  $3.08 \pm 0.16$ ,  $18.7 \pm 0.77$  and  $34.7 \pm 3.14$  pptv,  
3 respectively, accounting for 86%, 52%, 66%, 65% and 86% of the observed values at  
4 TMS during the same period, respectively. These results demonstrate that when there  
5 was mesoscale circulation, the alkyl nitrate levels at TMS were dominated by the  
6 photo-oxidation of their parent hydrocarbons that originated from the urban site TW.  
7 Although the mixing ratios of the parent hydrocarbons were lower at TMS, this is still  
8 one possible explanation leading to the similar levels of alkyl nitrates measured at the  
9 two sites.

10 For the “non-meso” scenario, the simulated levels of in-situ formation of  
11 MeONO<sub>2</sub>, EtONO<sub>2</sub>, 1-PrONO<sub>2</sub>, 2-PrONO<sub>2</sub> and 2-BuONO<sub>2</sub> at TMS were  $3.61 \pm 0.48$ ,  
12  $2.18 \pm 0.29$ ,  $1.03 \pm 0.13$ ,  $3.68 \pm 0.45$  and  $10.9 \pm 1.31$  pptv, respectively, accounting for  
13 18-42% of the observed C<sub>1</sub>-C<sub>4</sub> alkyl nitrates, indicating that other sources rather than  
14 local photochemical formation made significant contributions to ambient levels of  
15 alkyl nitrates. As stated earlier, TMS was a mountain site with sparse anthropogenic  
16 emissions nearby. However, the prevailing synoptic northerly winds in “non-meso”  
17 scenario suggested possible regional sources of alkyl nitrates from inland PRD region  
18 to the mountain site. The impact of regional transport on the variations of air  
19 pollutants at TMS for the days without mesoscale circulation, especially when the  
20 prevailing winds were from the north with high speeds, was corroborated in Guo et al.  
21 (2013a). By excluding the locally-formed alkyl nitrates from their overall levels, the  
22 contribution of regional sources to alkyl nitrates was determined for TMS. The  
23 regional source contributions to MeONO<sub>2</sub>, EtONO<sub>2</sub>, 1-PrONO<sub>2</sub>, 2-PrONO<sub>2</sub> and  
24 2-BuONO<sub>2</sub> were  $7.07 \pm 0.50$ ,  $8.44 \pm 0.62$ ,  $2.11 \pm 0.22$ ,  $16.86 \pm 1.17$ , and  $15.15 \pm 1.49$   
25 pptv, respectively, accounting for 58-82% of the alkyl nitrates measured at TMS. It is  
26 noteworthy that the regional alkyl nitrates included influences from all source  
27 categories (photochemical formation, biomass burning and oceanic emissions) for the  
28 inland PRD region.

1 Table 3. Mixing ratios of C<sub>1</sub>-C<sub>4</sub> alkyl nitrates influenced by mesoscale circulation  
 2 (“Meso”), in-situ formation and regional transport at TMS (unit: pptv).

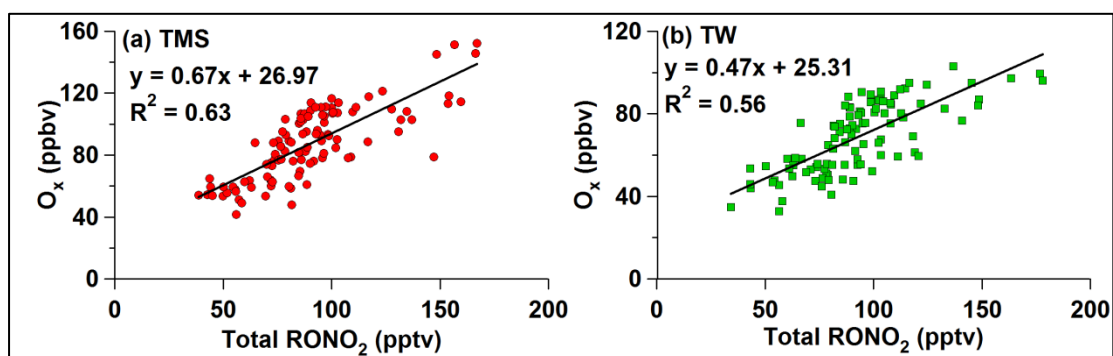
Scenario	MeONO <sub>2</sub>	EtONO <sub>2</sub>	1-PrONO <sub>2</sub>	2-PrONO <sub>2</sub>	2-BuONO <sub>2</sub>
“Meso”	9.97 ± 0.85	7.38 ± 0.44	3.08 ± 0.16	18.7 ± 0.77	34.7 ± 3.14
In-situ formation	3.61 ± 0.48	2.18 ± 0.29	1.03 ± 0.13	3.68 ± 0.45	10.9 ± 1.31
Regional transport	7.07 ± 0.50	8.44 ± 0.62	2.11 ± 0.22	16.86 ± 1.17	15.15 ± 1.49

3

### 4 **3.3. Relationship of alkyl nitrates with O<sub>3</sub>**

5 Alkyl nitrates are mainly formed through the reaction of peroxy radical (RO<sub>2</sub>)  
 6 and NO. However, NO can be oxidized by RO<sub>2</sub> to form NO<sub>2</sub>, which results in  
 7 tropospheric O<sub>3</sub> formation through NO<sub>2</sub> photolysis. Hence, investigating the  
 8 relationship between alkyl nitrates and O<sub>3</sub> is useful for evaluating the influence of  
 9 alkyl nitrates on O<sub>3</sub> formation (Simpson et al., 2006). Since photochemical formation  
 10 of O<sub>3</sub> and alkyl nitrates occurs during daytime hours, the relationship between O<sub>3</sub> and  
 11 alkyl nitrates is usually evaluated using the observed daytime data (*i.e.*, 0900-1600  
 12 LT). In this study, the “oxidant” O<sub>x</sub> (O<sub>3</sub> + NO<sub>2</sub>) was considered to be a better  
 13 representation of O<sub>3</sub> levels as it takes into account the effect of O<sub>3</sub> titration by NO.  
 14 Figure 11 shows the correlation between O<sub>x</sub> and the total alkyl nitrates (ΣRONO<sub>2</sub>) at  
 15 daytime hours. Good correlations were found at TMS (R<sup>2</sup> = 0.63) and TW (R<sup>2</sup> = 0.56)  
 16 with the slopes of 0.67 and 0.47 ppbv/pptv, respectively, suggesting that when 1 pptv  
 17 of total alkyl nitrates were formed from the reaction of RO<sub>2</sub> and NO, 0.67 and 0.47  
 18 ppbv of O<sub>x</sub> could be simultaneously produced at TMS and TW, respectively. The  
 19 relatively higher slope at TMS than at TW was owing to higher concentrations of HO<sub>x</sub>  
 20 radicals and higher photochemical reactivity of VOCs at TMS (Lyu et al., 2016).  
 21 Additionally, as the formation of alkyl nitrates consumes NO, this process results in a  
 22 negative contribution to O<sub>3</sub> formation. To quantify the negative influence on O<sub>3</sub>, the  
 23 PBM-MCM model was applied to the whole data collected at TMS and TW,  
 24 respectively (Lyu et al., 2016). The formation of alkyl nitrates made negative  
 25 contributions to the O<sub>3</sub> production, with the average reduction of 64.6 (TW: 24.9),  
 26 37.4 (11.0), 18.9 (2.6), 39.6 (11.1), and 115.1 (40.6) pptv of O<sub>3</sub> for the formation of

1 MeONO<sub>2</sub>, EtONO<sub>2</sub>, 1-PrONO<sub>2</sub>, 2-PrONO<sub>2</sub> and 2-BuONO<sub>2</sub> at TMS, respectively.  
2 Furthermore, moderate to good correlation was found between the simulated O<sub>3</sub>  
3 reduction and the photochemically formed alkyl nitrates at TMS (R<sup>2</sup> = 0.42) and TW  
4 (R<sup>2</sup> = 0.72), with the average O<sub>3</sub> reduction rate of 4.1 and 4.7 pptv/pptv, respectively.  
5 Namely, O<sub>3</sub> was reduced by 4.1 and 4.7 pptv if 1 pptv of alkyl nitrates were formed at  
6 TMS and TW, respectively.



7  
8 Figure 11. Correlation between O<sub>x</sub> (O<sub>3</sub> + NO<sub>2</sub>) and total alkyl nitrates at (a) TMS and  
9 (b) TW.

10  
11 Moreover, because secondary alkyl nitrates are formed through two main  
12 reaction pathways, “RO<sub>2</sub> + NO” and “RO + NO<sub>2</sub>”, it is of interest to investigate the  
13 relative contribution of the above pathways to the formation of alkyl nitrates. Two  
14 scenarios for model simulations were run and compared. The first scenario was the  
15 base case in which the model was run with all reaction pathways opened, while the  
16 second scenario was the constrained case in which the pathway of RO<sub>2</sub> + NO →  
17 RONO<sub>2</sub> was shut down. It was found that the reaction of “RO<sub>2</sub> + NO” was the  
18 prominent pathway for the secondary formation of alkyl nitrates at the two sites. The  
19 contributions of CH<sub>3</sub>O<sub>2</sub> + NO to MeONO<sub>2</sub> accounted for about 72% and 50% of the  
20 secondarily formed MeONO<sub>2</sub>, while the contributions of RO<sub>2</sub> + NO were 97-99 and  
21 95-99% of the secondarily formed C<sub>2</sub>-C<sub>4</sub> alkyl nitrates at TMS and TW, respectively.  
22 These results are similar to the findings obtained at Tai O, Hong Kong (Lyu et al.,  
23 2015). The lower contributions of RO<sub>2</sub> + NO to MeONO<sub>2</sub> at the two sites were related  
24 to the higher levels of CH<sub>3</sub>O from the oxidation of CH<sub>4</sub> and the decomposition of  
25 larger RO<sub>2</sub> radicals.

26

#### 1 **4. Conclusions**

2 Intensive field measurements of alkyl nitrates and their parent hydrocarbons  
3 were conducted concurrently at a mountain site (TMS) and an urban site (TW) at the  
4 base of the same mountain in Hong Kong from September to November 2010. The  
5 levels of MeONO<sub>2</sub>, EtONO<sub>2</sub> and 2-PrONO<sub>2</sub> were slightly higher at TW than at TMS  
6 ( $p < 0.05$ ), while the average mixing ratios of 1-PrONO<sub>2</sub> and 2-BuONO<sub>2</sub> were  
7 comparable at the two sites ( $p > 0.05$ ). However, the levels of the parent hydrocarbons  
8 of alkyl nitrates were lower at TMS, implying the complexity of sources of alkyl  
9 nitrates. Receptor model and photochemical box model simulations found that  
10 mesoscale circulation and regional transport had a significant impact on the levels of  
11 alkyl nitrates at the two sites. At TW, secondary formation was the dominant  
12 contributor to alkyl nitrates when there was mesoscale circulation, while the  
13 contributions of secondary formation and biomass burning were comparable under the  
14 influence of regional transport. At TMS, photo-oxidation of the parent hydrocarbons  
15 from TW contributed 52-85% to the ambient levels of alkyl nitrates on the days with  
16 mesoscale circulations between the two sites. On the other hand, alkyl nitrates from  
17 the inland PRD region were responsible for 58-82% of the observed values at TMS on  
18 the days with regional influence. The photo-oxidation of parent hydrocarbons from  
19 TW and regional transport resulted in similar values of alkyl nitrates observed at the  
20 two sites. With regard to the secondarily formed alkyl nitrates, the reaction of RO<sub>2</sub>  
21 and NO was the prominent pathway at both sites. Moreover, the formation of alkyl  
22 nitrates made negative contributions to the O<sub>3</sub> formation, with a reduction rate of 4.1  
23 and 4.7 pptv O<sub>3</sub> per pptv alkyl nitrates at TMS and TW, respectively. The findings of  
24 this study will aid in understanding the source contributions and photochemical  
25 formation pathways of alkyl nitrates in Hong Kong's mountainous areas.

#### 26 **Acknowledgements**

27 This project was supported by the Research Grants Council of the Hong Kong Special  
28 Administrative Region via grants PolyU5154/13E, PolyU152052/14E and  
29 CRF/C5022-14G. This study was partly supported by the internal grants of the Hong  
30

1 Kong Polytechnic University (4-BCAV and 1-ZVCX), and the National Natural  
2 Science Foundation of China (No. 41405112 and 41275122). The challenging but  
3 ultimately very helpful comments of the anonymous reviewers are greatly  
4 appreciated.

## 5 **References**

- 6 AFCD (Agriculture, Fisheries and Conservation Department), 2008. Available at website:  
7 <http://www.afcd.gov.hk/>.
- 8 AFCD (Agriculture, Fisheries and Conservation Department), useful statistics, Last Review Date  
9 02 June 2015. Available at website: [http://www.afcd.gov.hk/english/country/cou\\_lea/  
10 cou\\_lea\\_use/cou\\_lea\\_use.html](http://www.afcd.gov.hk/english/country/cou_lea/cou_lea_use/cou_lea_use.html).
- 11 Archibald, A.T., Khan, M.A.H., Watson, L.A., Utembe, S.R., Shallcross, D.E., Clemmshaw, K.C.,  
12 Jenkin, M.E., 2007. Comment on 'Long-term atmospheric measurements of C<sub>1</sub>-C<sub>5</sub> alkyl  
13 nitrates in the Pearl River Delta region of southeast China' by Simpson et al. *Atmospheric  
14 Environment* 41, 7369-7370.
- 15 Arey, J., Aschmann, S.M., Kwok, E.S.C., Atkinson, R., 2001. Alkyl nitrate, hydroxyl nitrate, and  
16 hydroxycarbonyl formation from the NO<sub>x</sub>-air photooxidations of C<sub>5</sub>-C<sub>8</sub> n-alkanes. *Journal  
17 of Physical Chemistry* 105, 1020-1027.
- 18 Atkinson, R., Baulch, D.L., Cox, R.A., Crowley, J.N., Hampson, R.F., Hynes, R.G., Jenkin, M.E.,  
19 Rossi, M.J., Troe, J., Subcommittee, I., 2006. Evaluated kinetic and photochemical data for  
20 atmospheric chemistry: volume II – gas phase reactions of organic species. *Atmospheric  
21 Chemistry and Physics* 6, 3625-4055.
- 22 Barletta, B., Meinardi, S., Simpson, I.J., Atlas, E.L., Beyersdorf, A.J., Baker, A.K., Blake, N.J.,  
23 Yang, M., Midyett, J.R., Novak, B.J., Mckeachie, R.J., Fuelberg, H.E., Sachse, G.W., Avery,  
24 M.A., Campos, T., Weinheimer, A.J., Rowland, F.S., Blake, D.R., 2009. Characterization of  
25 volatile organic compounds (VOCs) in Asian and north American pollution plumes during  
26 INTEX-B: identification of specific Chinese air mass tracers. *Atmospheric Chemistry and  
27 Physics* 9, 5371-5388.
- 28 Barletta, B., Meinardi, S., Simpson, I.J., Khwaja, H.A., Blake, D.R., Rowland, F.S., 2002. Mixing  
29 ratios of volatile organic compounds (VOCs) in the atmosphere of Karachi, Pakistan.  
30 *Atmospheric Environment* 36, 3429-3443.
- 31 Bertman, S.B., Roberts, J.M., Parrish, D.D., Buhr, M.P., Goldan, P.D., Kuster, W.C., Fehsenfeld,  
32 F.C., Montzka, S.A., Westberg, H., 1995. Evolution of alkyl nitrates with air mass age.  
33 *Journal of Geophysical Research* 100, 22805-22813.
- 34 Blake, N.J., D. R. Blake, A. L. Swanson, E. Atlas, F. Flocke, and F. S. Rowland, 2003. Latitudinal,  
35 vertical, and seasonal variations of C<sub>1</sub>-C<sub>4</sub> alkyl nitrates in the troposphere over the Pacific  
36 Ocean during PEM-Tropics A and B: Oceanic and continental sources, *Journal of  
37 Geophysical Research* 108(D2), 8242, doi:10.1029/2001JD001444, 2003.

1 Clemitshaw, K.C., Williams, J., Rattigan, O.V., Shallcross, D.E., Law, K.S., Cox, R.A., 1997.  
2 Gas-phase ultraviolet absorption cross-sections and atmospheric lifetimes of several C<sub>2</sub>–C<sub>5</sub>  
3 alkyl nitrates. *Journal of Photochemistry and Photobiology A: Chemistry* 102, 117–126.

4 Gao, J., Wang, T., Ding, A.J., Liu, C.B., 2005. Observation study of ozone and carbon monoxide  
5 at the summit of mount Tai (1534 m a.s.l.) in central-eastern China. *Atmospheric*  
6 *Environment* 39, 4779-4791.

7 Guo, H., Jiang, F., Cheng, H.R., Simpson, I.J., Wang, X.M., Ding, A.J., Wang, T.J., Saunders, S.M.,  
8 Wang, T., Lam, S.H.M., Blake, D.R., Zhang, Y.L., Xie, M., 2009. Concurrent observations of  
9 air pollutants at two sites in the Pearl River Delta and the implication of regional transport.  
10 *Atmospheric Chemistry and Physics* 9, 7343-7360.

11 Guo, H., Cheng, H.R., Ling, Z.H., Louie, P.K.K., Ayoko, G.A., 2011. Which emission sources are  
12 responsible for the volatile organic compounds in the atmosphere of Pearl River Delta?  
13 *Journal of Hazardous Materials* 188, 116-124.

14 Guo, H., Ling, Z.H., Cheung, K., Jiang, F., Wang, D.W., Simpson, I.J., Barletta, B., Meinardi, S.,  
15 Wang, T.J., Wang, X.M., Saunders, S.M., Blake, D.R., 2013a. Characterization of  
16 photochemical pollution at different elevations in mountainous areas in Hong Kong.  
17 *Atmospheric Chemistry and Physics* 13, 3881-3898.

18 Guo, H., Ling, Z.H., Cheung, K., Wang, D.W., Simpson, I.J., Blake, D.R., 2013b. Acetone in the  
19 atmosphere of Hong Kong: Abundance, sources and photochemical precursors. *Atmospheric*  
20 *Environment* 65, 80-88.

21 Guo, H., Ling, Z.H., Simpson, I.J., Blake, D.R., Wang, D.W., 2012. Observations of isoprene,  
22 methacrolein (MAC) and methyl vinyl ketone (MVK) at a mountain site in Hong Kong.  
23 *Journal of Geophysical Research* 117, doi:10.1029/2012JD017750.

24 HKCSD (Hong Kong Census and Statistics Department), 2010. Hong Kong Energy Statistics:  
25 Annual Report. <http://www.censtatd.gov.hk>.

26 HKEPD (Hong Kong Protection Department), 2012. Air Quality in Hong Kong.  
27 2011. <http://www.epd-asg.gov.hk/english/report/aqr.html>.

28 Jenkin, M. E., Saunders, S. M., Wagner, V., and Pilling, M. J., 1997. The tropospheric degradation  
29 of volatile organic compounds: A protocol for mechanism development. *Atmospheric*  
30 *Environment* 31, 81-107, 1997.

31 Jenkin, M. E., Saunders, S. M., Wagner, V., and Pilling, M. J., 2003. Protocol for the development  
32 of the master chemical mechanism MCMv3 (Part B): Tropospheric degradation of aromatic  
33 volatile organic compounds, *Atmospheric Chemistry and Physics* 3, 181-193, 2003.

34 Jenkin, M.E., Clemitshaw, C., 2000. Ozone and other secondary photochemical pollutants:  
35 Chemical processes governing their formation in the planetary boundary layer. *Atmospheric*  
36 *Environment* 34, 2499-2527.

37 Jiang, F., Guo, H., Wang, T.J., Cheng, H.R., Wang, X.M., Simpson, I.J., Ding, A.J., Saunders, S.M.,  
38 Lam, S.H.M., Blake, D.R., 2010. An O<sub>3</sub> episode in the Pearl River Delta: field observation  
39 and model simulation. *Journal of Geophysical Research* 115, doi:/10.1029/2009JD013583.

- 1 Kwok, E.S.C. and Atkinson, R., 1995. Estimation of hydroxyl radical reaction-rate constants for  
2 gas-phase organic-compounds using a structure-reactivity relationship-an update.  
3 *Atmospheric Environment* 29, 1685-1695.
- 4 Lam, S.H.M., Saunders, S.M., Guo, H., Ling, Z.H., Jiang, F., Wang, X.M., Wang, T.J., 2013.  
5 Modelling VOC source impacts on high ozone episode days observed at a mountain summit  
6 in Hong Kong under the influence of mountain-valley breezes. *Atmospheric Environment* 81,  
7 166-176.
- 8 Lau, A. K.H., Yuan, Z.B., Yu, J.Z., Louie, P.K.K., 2010. Source apportionment of ambient volatile  
9 organic compounds in Hong Kong. *Science of the Total Environment* 408, 4138-4149.
- 10 Ling, Z.H. and Guo, H., 2014. Contribution of VOC sources to photochemical ozone formation  
11 and its control policy implication in Hong Kong. *Environmental Science and Policy* 38,  
12 180-191.
- 13 Ling, Z.H., Guo, H., Cheng, H.R., Yu, Y.F., 2011. Sources of ambient volatile organic compounds  
14 and their contributions to photochemical ozone formation at a site in the Pearl River Delta,  
15 southern China. *Environmental Pollution* 159, 2310-2319.
- 16 Ling, Z.H., Guo, H., Lam, S.H.M., Saunders, S.M., Wang, T., 2014. Atmospheric photochemical  
17 reactivity and ozone production at two sites in Hong Kong: Application of a Master Chemical  
18 Mechanism-photochemical box model. *Journal of Geophysical Research* 119,  
19 doi:10.1002/2014JD021794.
- 20 Lyu, X.P., Ling, Z.H., Guo, H., Zeng, L.W., Wang, N., 2016. Impact of alkyl nitrate chemistry on  
21 photochemical reactivity and O<sub>3</sub> production in Hong Kong. In preparation.
- 22 Lyu, X.P., Ling, Z.H., Guo, H., Saunders, S.M., Lam, S.H.M., Wang, N., Wang, Y., Liu, M., Wang,  
23 T., 2015. Re-examination of C<sub>1</sub>-C<sub>5</sub> alkyl nitrates in Hong Kong using an observation-based  
24 model. *Atmospheric Environment* 120, 28-37.
- 25 Marandino, C.A., Tegtmeier, S., Krüger, K., Zindler, C., Atlas, E.L., Moore, F., Bange, H.W., 2013.  
26 Dimethylsulphide (DMS) emissions from the western Pacific Ocean: a potential marine  
27 source for stratospheric sulphur? *Atmospheric Chemistry and Physics* 13, 8427-8437.
- 28 Paatero, P., 2000. User's guide for Positive Matrix Factorization Programs PMF2 and PMF3, part  
29 1: Tutorial. Prepared by University of Helsinki, Finland (February).
- 30 Pinho, P.G., Lemos, L.T., Pio, C.A., Evtugina, M.G., Nunes, T.V., Jenkin, M.E., 2009. Detailed  
31 chemical analysis of regional-scale air pollution in western Portugal using an adapted version  
32 of MCM v3.1. *Science of the Total Environment* 407, 2024-2038.
- 33 Reeves, C.E., Slemr, J., Oram, D.E., Worton, D., Penkett, S.A., Stewart, D.J., Purvis, R., Watson,  
34 N., Hopkins, J., Lewis, A., Methven, J., Blake, D.R., Atlas, E., 2007. Alkyl nitrates in outflow  
35 from North America over the North Atlantic during intercontinental transport of ozone and  
36 precursors 2004. *Journal of Geophysical Research* 112, D10S037, doi:  
37 10.1029/2006JD007567.
- 38 Roberts, J.M., Bertman, S.B., Parrish, D.D., Fehsenfeld, F.C., Johnson, B.T., Niki, H., 1998.  
39 Measurements of alkyl nitrates at Chebogue Point Nova Scotia during the 1993 North



1 Atlantic Regional Experiment (NARE) intensive. *Journal of Geophysical Research* 103 (D11),  
2 13569-13580.

3 Russo, R.S., Zhou, Y., Haase, K.B., Wingenter, O.W., Frinak, E.K., Mao, H., Talbot, R.W., Sive,  
4 B.C., 2010. Temporal variability, sources and sinks of C<sub>1</sub>-C<sub>5</sub> alkyl nitrates in coastal New  
5 England. *Atmospheric Chemistry and Physics* 10, 1865-1883.

6 Saunders, S. M., Jenkin, M. E., Derwent, R. G., and Pilling, M. J., 2003. Protocol for the  
7 development of the master chemical mechanism MCMv3 (Part A): Tropospheric degradation  
8 of non-aromatic volatile organic compounds. *Atmospheric Chemistry and Physics* 3,  
9 161-180.

10 Seinfeld, J.H. and Pandis, S.N., 2006. *Atmospheric Chemistry and Physics: from air pollution to*  
11 *climate change*, 2nd edition. Wiley Publisher, New Jersey, USA.

12 Simpson, I.J., Akagi, S.K., Barletta, B., Blake, N.J., Choi, Y., Diskin, G.S., Fried, A., Fuelberg,  
13 H.E., Meinardi, S., Rowland, F.S., Vay, S.A., Weinheimer, A.J., Wennberg, P.O., Wiebring, P.,  
14 Wisthaler, A., Yang, M., Yokelson, R.J., Blake, D.R., 2011. Boreal forest fire emissions in  
15 fresh Canadian smoke plumes: C<sub>1</sub>-C<sub>10</sub> volatile organic compounds (VOCs), CO<sub>2</sub>, CO, NO<sub>2</sub>,  
16 NO, HCN and CH<sub>3</sub>CN. *Atmospheric Chemistry and Physics* 11, 6445–6463.

17 Simpson, I.J., Blake, N.J., Barletta, B., Diskin, G.S., Fuelberg, H.E., Gorham, K., Huey, L.G.,  
18 Meinardi, S., Rowland, F.S., Vay, S.A., Weinheimer, A.J., Yang, M., Blake, D.R., 2010.  
19 Characterization of trace gases measured over Alberta oil sands mining operations: 76  
20 speciated C<sub>2</sub>-C<sub>10</sub> volatile organic compounds (VOCs), CO<sub>2</sub>, CH<sub>4</sub>, CO, NO, NO<sub>2</sub>, NO<sub>y</sub>, O<sub>3</sub> and  
21 SO<sub>2</sub>. *Atmospheric Chemistry and Physics* 10, 11931-11954.

22 Simpson, I.J., Blake, N.J., Blake, D.R., Atlas, E., Flocke, F., Crawford, J.H., Fuelberg, H.E., Kiley,  
23 C.M., Meinardi, S., Rowland, F.S., 2003. Photochemical production and evolution of selected  
24 C<sub>2</sub>-C<sub>5</sub> alkyl nitrates in tropospheric air influenced by Asia outflow. *Journal of Geophysical*  
25 *Research* 108, D20, doi:10.1029/2002JD002830.

26 Simpson, I.J., Meinardi, S., Blake, D.R., Blake, N.J., 2002. A biomass burning source of C<sub>1</sub>-C<sub>4</sub>  
27 alkyl nitrates. *Geophysical Research Letters* 29 (24), 2168, doi: 10.1029/2002GL016290.

28 Simpson, I.J., Wang, T., Guo, H., Kwok, Y.H., Flocke, F., Atlas, E., Meinardi, S., Rowland, F.S.,  
29 Blake, D.R., 2006. Long-term atmospheric measurements of C<sub>1</sub>-C<sub>5</sub> alkyl nitrates in the Pearl  
30 River Delta region of southeast China. *Atmospheric Environment* 40, 1619-1632.

31 Sommariva, R., Trainer, M., de Gouw, J.A., Roberts, J.M., Warneke, C., Atlas, E., Flocke, F.,  
32 Goldan, P.D., Kuster, W.C., Swanson, A.L., Fehsenfeld, F.C., 2008. A study of organic  
33 nitrates formation in an urban plume using a Master Chemical Mechanism. *Atmospheric*  
34 *Environment* 42, 5771-5786.

35 Talukdar, R.K., Burkholder, J.B., Hunter, M., Gilles, M.K., Roberts, J.M., Ravishankara, A.R.,  
36 1997. Atmospheric fate of several alkyl nitrates Part 2 UV absorption cross-sections and  
37 photodissociation quantum yields. *Journal of the Chemical Society, Faraday Transactions* 93,  
38 2797–2805.

39 Wang, M., Shao, M., Chen, W.T., Lu, S.H., Wang, C., Huang, D.K., Yuan, B., Zeng, L.M., Zhao,

1 Y., 2013. Measurements of C<sub>1</sub>-C<sub>4</sub> alkyl nitrates and their relationships with carbonyl  
2 compounds and O<sub>3</sub> in Chinese cities. *Atmospheric Environment* 81, 389-398.

3 Wang, T., Poon, C.N., Kwok, Y.H., Li, Y.S., 2003. Characterizing the temporal variability and  
4 emission patterns of pollution plumes in the Pearl River Delta of China. *Atmospheric*  
5 *Environment* 37, 3539-3550.

6 Wang, T., Wong, H.L.A., Tang, J., Ding, A., Wu, W.S., Zhang, X.C., 2006. On the origin of surface  
7 ozone and reactive nitrogen observed at a remote site in the northeastern Qinghai-Tibetan  
8 Plateau, western China. *Journal of Geophysical Research* 111, D08303, doi:  
9 10.1029/2005JD006527.

10 Worton, D.R., Reeves, C.E., Penkett, S.A., Sturges, W.T., Slemr, J., Oram, D.E., Bandy, B.J.,  
11 Bloss, W.J., Carslaw, N., Davey, J., Emmerson, K.M., Gravestock, T.J., Hamilton, J.F., Heard,  
12 D.E., Hopkins, J.R., Hulse, A., Ingram, T., Jacob, M.J., Lee, J.D., Leigh, R.J., Lewis, A.C.,  
13 Monks, P.S., Smith, S.C., 2010. Alkyl nitrate photochemistry during the tropospheric organic  
14 chemistry experiment. *Atmospheric Environment* 44, 773-785.

15 Wu, Z.Y., Wang, X.M., Chen, F., Turnipseed, A.A., Guenther, A., Niyogi, D., Charusombat, U.,  
16 Xia, B.C., Munger, J.W., Alapty, K., 2011. Evaluating the calculated dry deposition velocities  
17 of reactive nitrogen oxides and ozone from two community models over a temperate  
18 deciduous forest. *Atmospheric Environment* 45, 2633-2674.

19 Yuan, B., Liu, Y., Shao, M., Lu, S.H., Streets, D.G., 2010. Biomass burning contributions to  
20 ambient VOCs species at a receptor site in the Pearl River Delta (PRD), China.  
21 *Environmental Science and Technology* 44, 4577-4582.

22

23

24